Type of file: PDF
Title of file for HTML: Supplementary Information
Description: Supplementary Figures and Supplementary Tables.

Type of file: PDF
Title of file for HTML: Peer Review File
Description:

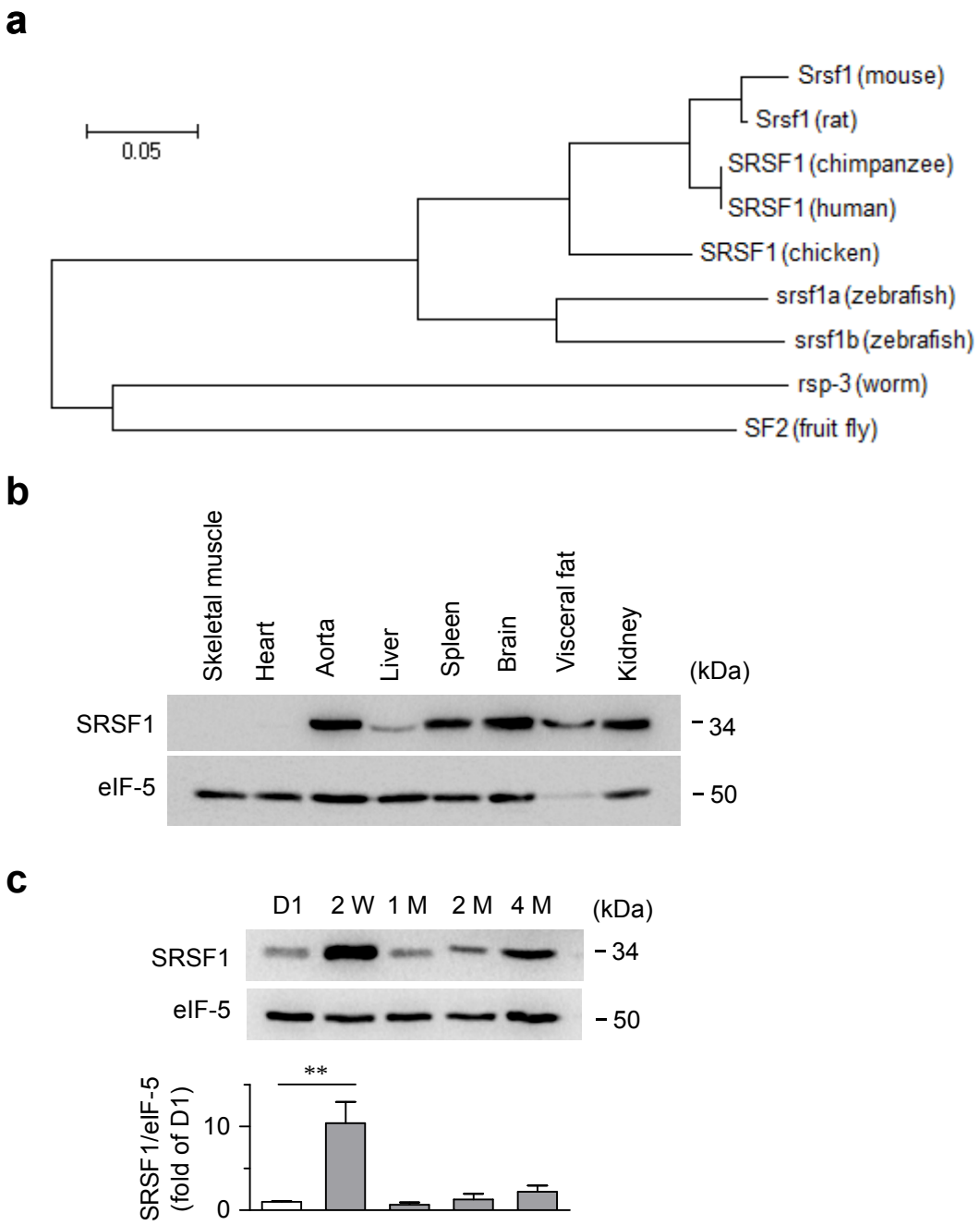

Supplementary Figure 1 | Expression profile of Srsf1 in aorta. (**a**) Molecular phylogenetic tree of SRSF1 in selected model organisms. The branch length shows the distance as measured by the average nucleotide substitutions per site. (**b**) Representative western blots showing that SRSF1 is expressed in the aorta in 12-14 week-old rats. (**c**) Western blots and analysis of aortic SRSF1 expression at birth (D1), two weeks (2 W), one month (1 M), two months (2 M), and four months (4 M) after birth; n = 5 per group. eIF-5 served as internal control. $^{**}P$ <0.01, one-way ANOVA (**c**). Data are mean ± s.e.m. of four (**c**) independent experiments.

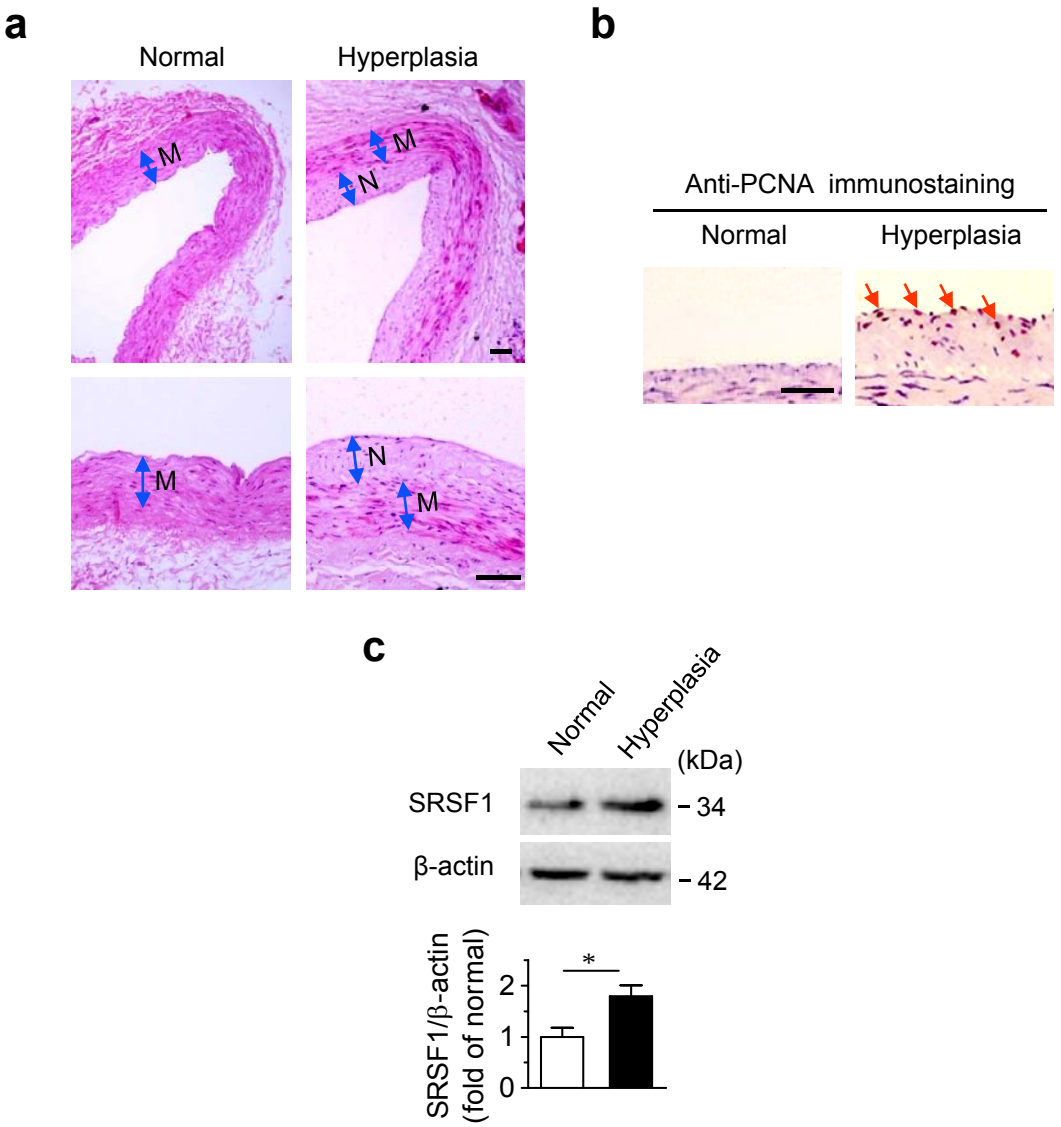

Supplementary Figure 2 | Increased SRSF1 protein in hyperplasia human artery. (**a**) Representative photomicrographs of hematoxylin/eosin staining of the neointima area of human internal mammary arteries (N, neointima; M, media) collected during cardiac bypass surgery (×100; scale bars, 50 μm). (**b**) Representative photomicrographs of immunohistochemical staining showing PCNA-positive cells in a human artery with hyperplasia (scale bar, 25 μm). Arrows indicate PCNA-positive cells (dark brown). (**c**) Representative western blots and averaged data showing the SRSF1 levels in human arteries; n = 5 per group. *P<0.05, Student's t-test (**c**). Data are mean ± s.e.m. of three independent experiments (**c**).

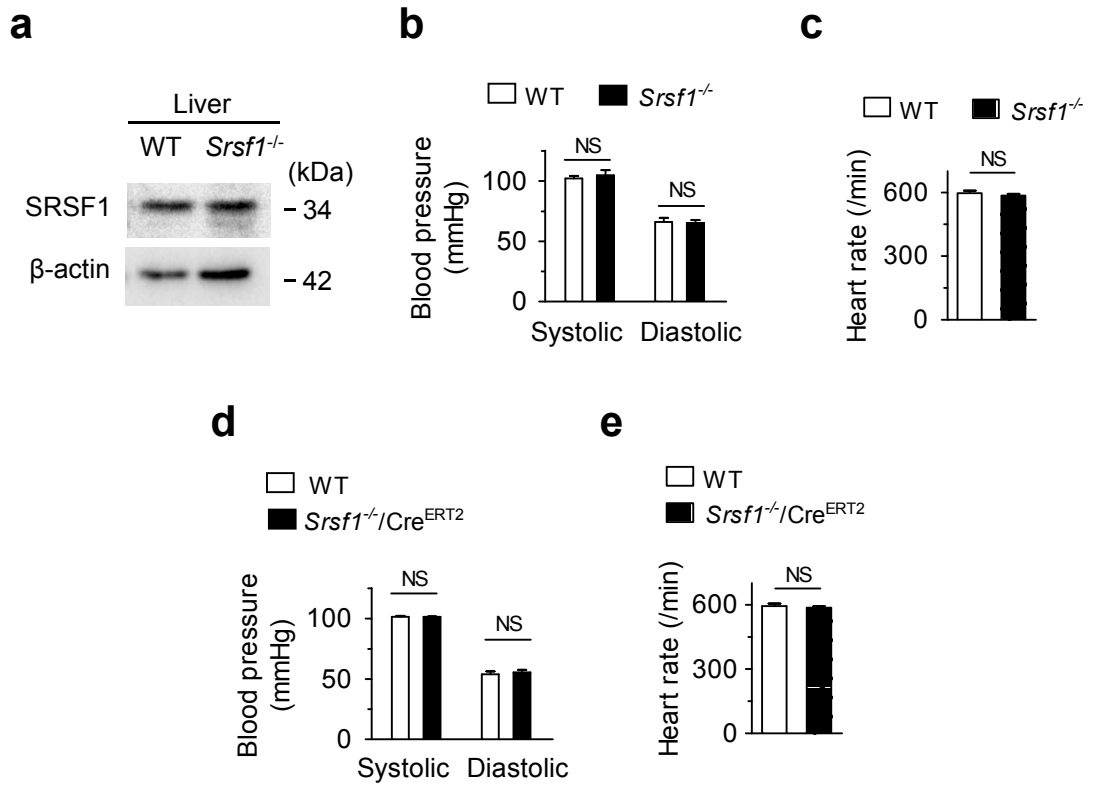

Supplementary Figure 3 | Genotyping and blood pressure of smooth muscle cell-specific *Srsf1* knockout (*Srsf1*$^{-/-}$) mice and inducible smooth muscle cell-specific *Srsf1* knockout (*Srsf1*$^{-/-}$/Cre^{ERT2}) mice. (**a**) Representative western blots demonstrating the unaltered expression of SRSF1 at the protein level in liver of WT and *Srsf1*$^{-/-}$ mice. (**b**,**c**) Systolic and diastolic blood pressure (**b**), and heart rate (**c**) of WT and *Srsf1*$^{-/-}$mice at 10 weeks of age; *n* = 10 per group. (**d**,**e**) Systolic and diastolic blood pressure (**d**), and heart rate (**e**) of WT and *Srsf1*$^{-/-}$/Cre^{ERT2} at 10 weeks of age; *n* = 12 per group. NS, not significant, Student's *t*-test (**b**-**e**).

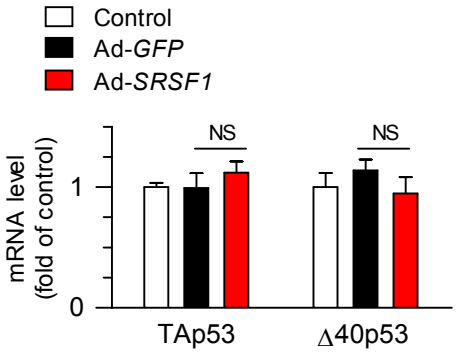

Supplementary Figure 4 | SRSF1 overexpression did not affect the expression of full-length p53 and Δ40p53. There are at least 3 subclasses of human p53 isoforms due to N-terminal truncation, TAp53 (N-terminal with completely conserved transactive domain), Δ40p53 (truncated N-terminal missing the first 39 amino-acids), and Δ133p53 (truncated N-terminal missing the first 132 amino-acids). 'Δ40p53' primers qualify the Δ40p53 isoform subclass; 'TAp53' primers qualify the Δ40p53 isoform subclass and the TAp53 isoform subclass (mainly includes full-length p53). Real-time PCR showing the mRNA levels of the TAp53 and Δ40p53 isoforms in HASMCs infected with Ad-*GFP* or Ad-*SRSF1* (m.o.i. 100, 48 h); *n* = 8 per group. NS, not significant, one-way ANOVA. Data are mean ± s.e.m. of four independent experiments.

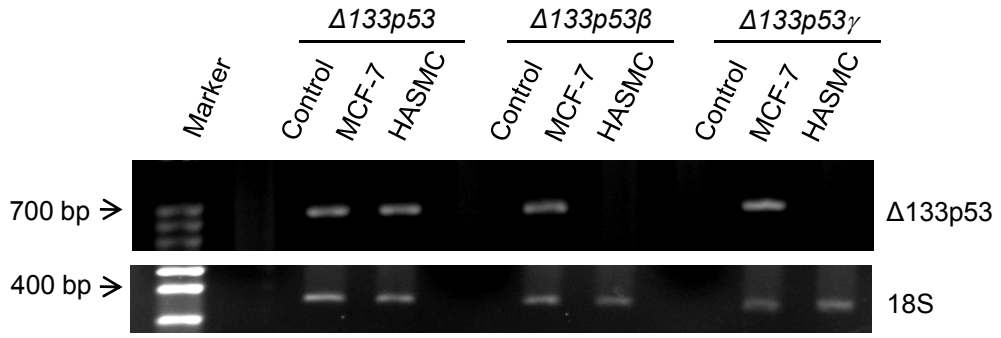

Supplementary Figure 5 | Amplification of Δ133p53 isoform mRNAs by nested PCR in human cells. MCF-7, human breast adenocarcinoma cell line, positive control; HASMC, human aortic smooth muscle cell; Con, negative control, ddH_2O was used instead of cDNA. Specific primers were used for amplifying *Δ133p53* (*Δ133p53α*), *Δ133p53β* or *Δ133p53γ* by nested RT-PCR (see Supplementary Tables 6 and 7). PCR products (20 μL) were migrated on 1% agarose gel. Marker, 100 bp DNA ladder. DNA sequencing of the bands obtained was performed to verify the isoforms. While all three *Δ133p53* isoforms (α, β and γ) present in MCF-7 cells, only Δ133p53α was detectable in HASMCs.

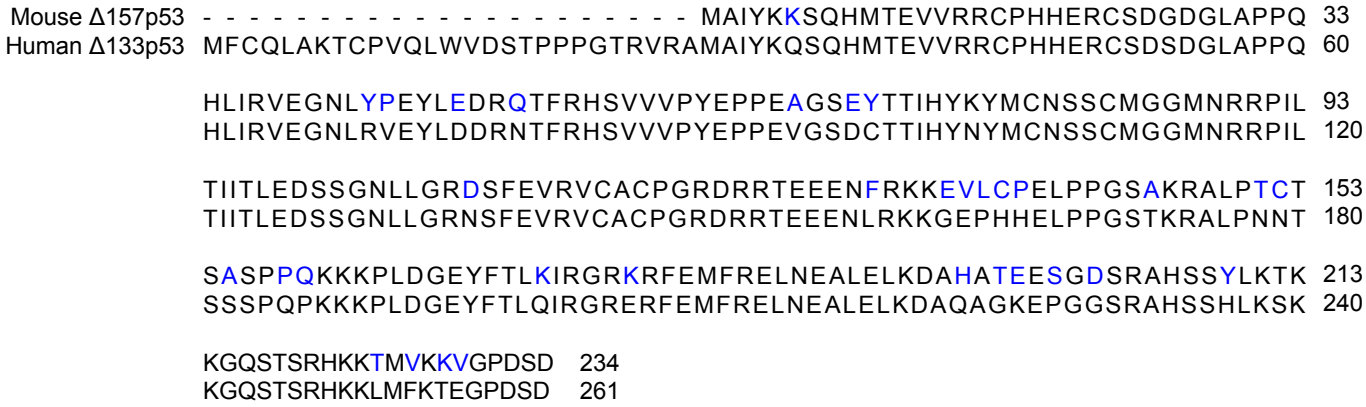

Supplementary Figure 6 | Protein alignment between human Δ133p53 and mouse Δ157p53 (named MΔ133p53 in this study) illustrating the high degree of homology between the two protein sequences.

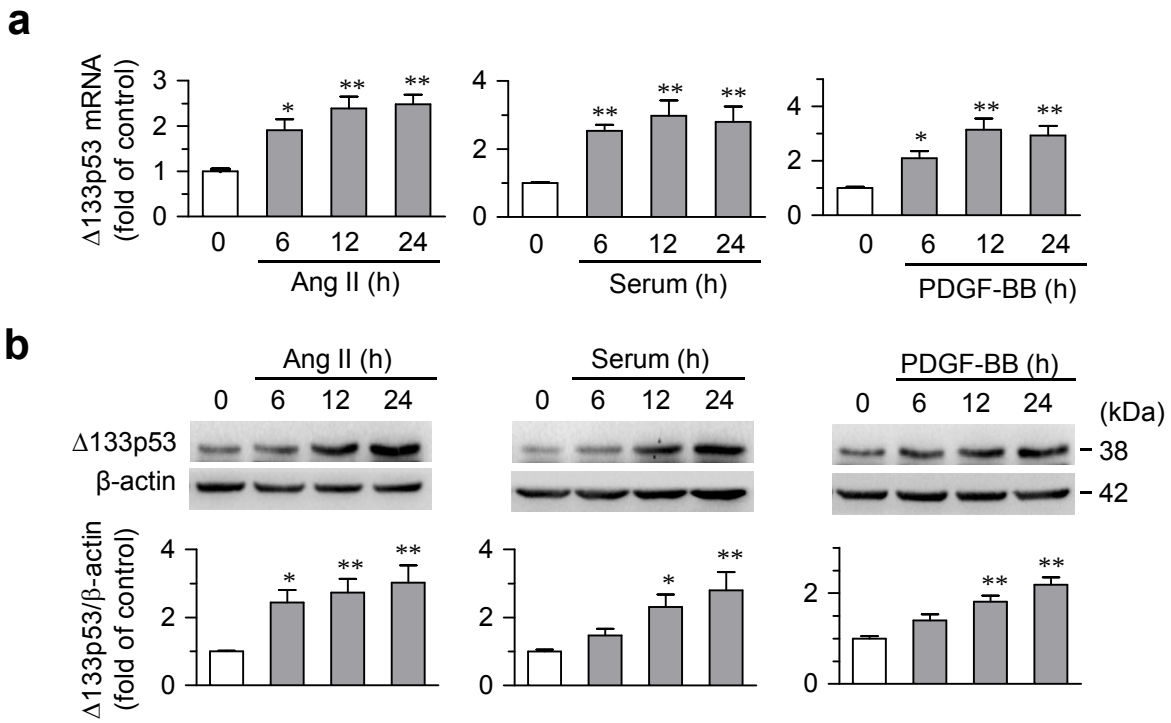

Supplementary Figure 7 | Δ133p53 expression was increased in proliferating smooth muscle cells. (**a**) Real-time PCR data showing the mRNA levels of Δ133p53 in HASMCs treated with Ang II (200 nM), serum (10% FBS), or PDGF-BB (10 μg/L) at 6, 12, and 24 h; *n* = 8 per group. (**b**) Representative western blots and averaged data showing the Δ133p53 levels in HASMCs treated as in (**a**); *n* = 7 per group. **P* <0.05, ***P* <0.01 *vs* control group, one-way ANOVA. Data are mean ± s.e.m. of five independent experiments.

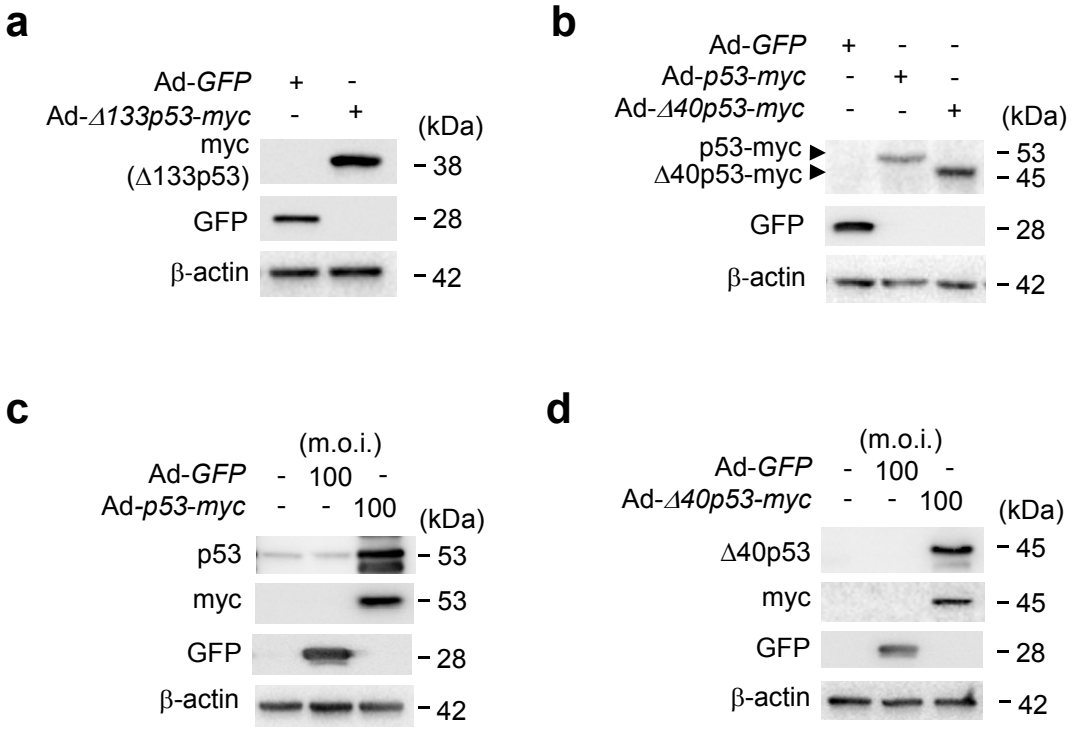

Supplementary Figure 8 | Representative western blots showing expression of indicated genes in rat carotid arteries at 4 days after Ad-*Δ133p53-myc* (**a**), Ad-*p53-myc* or Ad-*Δ40p53-myc* (**b**) delivery (*n* = 5 per group). (**c**,**d**) Representative western blots showing the p53 (**c**) or Δ40p53 (**d**) expression in cultured HASMCs infected with Ad-*GFP*, Ad-*p53*, or Ad-*Δ40p53* for 48 h (m.o.i. 100, *n* = 5 per group).

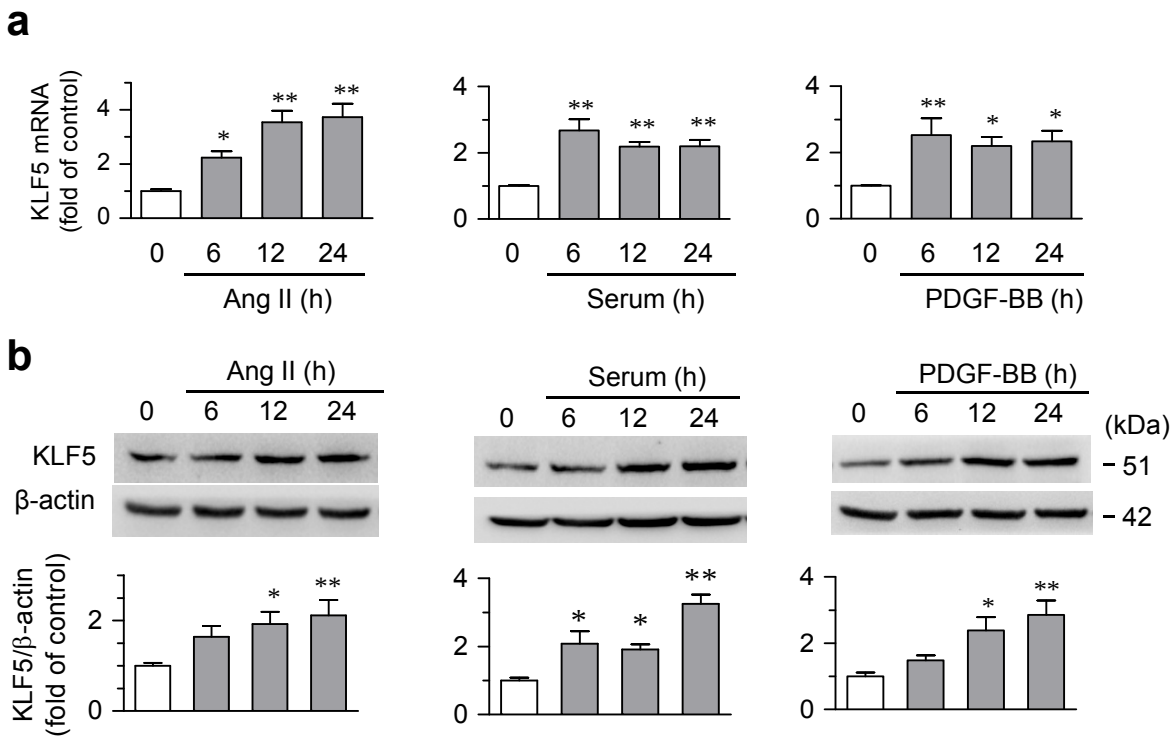

Supplementary Figure 9 | KLF5 expression was increased in proliferating smooth muscle cells. (**a**) Real-time PCR data showing the mRNA levels of KLF5 in HASMCs treated with Ang II (200 nM), serum (10% FBS), or PDGF-BB (10 μg L^{-1}) at 6, 12, and 24 h; *n* = 8 per group. (**b**) Representative western blots and averaged data showing KLF5 levels in HASMCs treated as in (**a**); *n* = 7 per group. **P* <0.05, ***P* <0.01 *vs* control group, one-way ANOVA. Data are mean ± s.e.m. of four independent experiments.

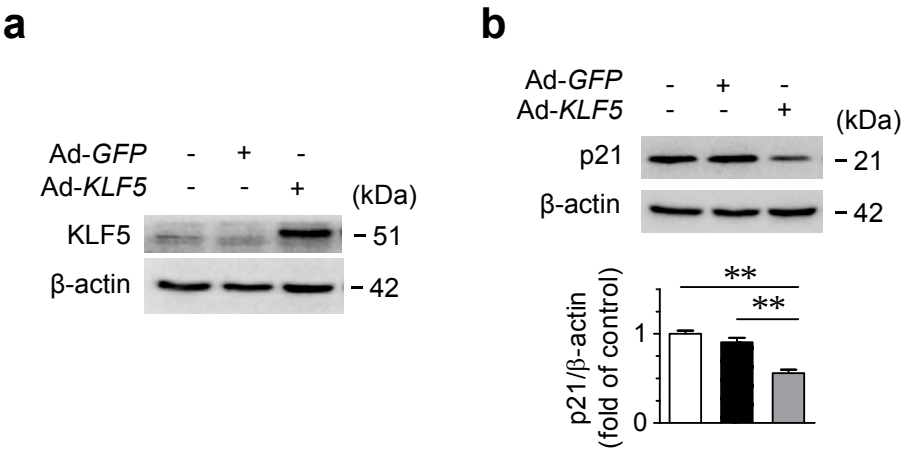

Supplementary Figure 10 | KLF5 decreased p21 expression. (**a**) Representative western blots showing the KLF5 expression in HASMCs infected with Ad-*GFP* or Ad-*KLF5* (m.o.i. 100, 48 h) (*n* = 5 per group). (**b**) Representative western blots and averaged data showing p21 levels in HASMCs treated as in (**a**); *n* = 5 per group. ***P* <0.01, one-way ANOVA (**b**). Data are mean ± s.e.m. of four independent experiments.

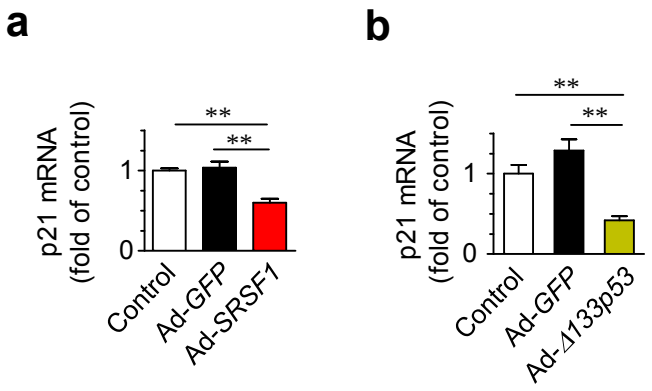

Supplementary Figure 11 | Overexpression of SRSF1 or Δ133p53 decreased p21 expression. (**a**) Real-time PCR data showing the mRNA levels of p21 in HASMCs infected with Ad-*SRSF1*; *n* = 7 per group. (**b**) Real-time PCR data showing the mRNA levels of p21 in HASMCs infected with Ad-*Δ133p53*; *n* = 12 per group. ***P* <0.01, one-way ANOVA. Data are mean ± s.e.m. of five independent experiments.

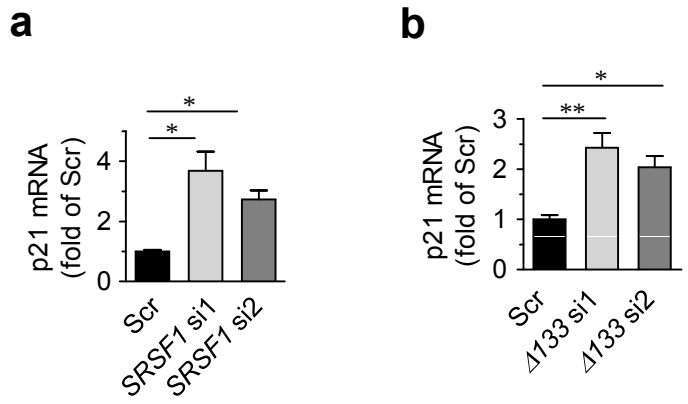

Supplementary Figure 12 | Knockdown of SRSF1 or Δ133p53 increased p21 expression. (**a**) Real-time PCR data showing the mRNA levels of p21 in HASMCs infected with scrambled or *SRSF1* siRNAs (*SRSF1* si1 and *SRSF1* si2); *n* = 8 per group. (**b**) Real-time PCR data showing the mRNA levels of p21 in HASMCs infected with scrambled or *Δ133p53* siRNAs (*Δ133* si1 and *Δ133* si2); *n* = 7 per group. Scr indicates scrambled siRNA control. **P* <0.05, ***P* <0.01, one-way ANOVA. Data are mean ± s.e.m. of five independent experiments.

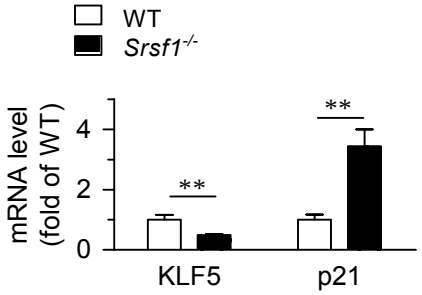

Supplementary Figure 13 | Real-time PCR data showing the mRNA levels of KLF5 and p21 in arteries from WT and *Srsf1*$^{-/-}$ mice; n = 8 per group. **P <0.01, Student's t-test. Data are mean ± s.e.m. of three independent experiments.

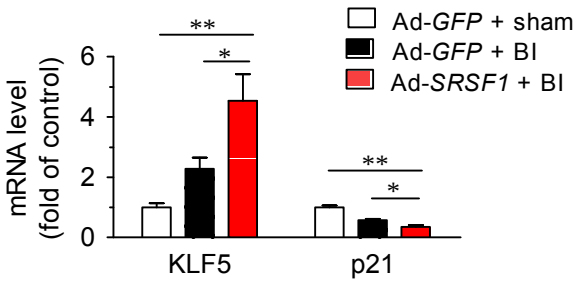

Supplementary Figure 14 | Real-time PCR data showing the mRNA levels of KLF5 and p21 in rat carotid arteries transfected with Ad-*GFP* or Ad-*SRSF1*, one week after balloon injury; n = 8/group. **P* <0.05, ***P* <0.01, one-way ANOVA. Data are mean ± s.e.m. of five independent experiments.

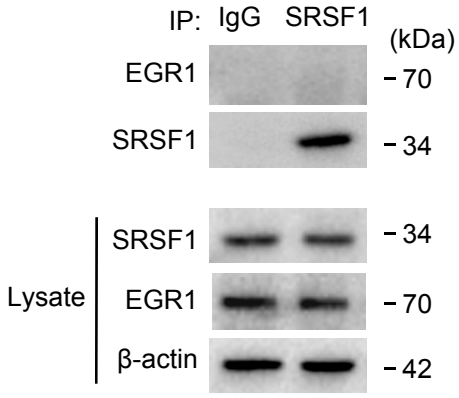

Supplementary Figure 15 | Representative western blots of co-immunoprecipitation between SRSF1 and EGR1 in HASMCs (*n* = 5).

a

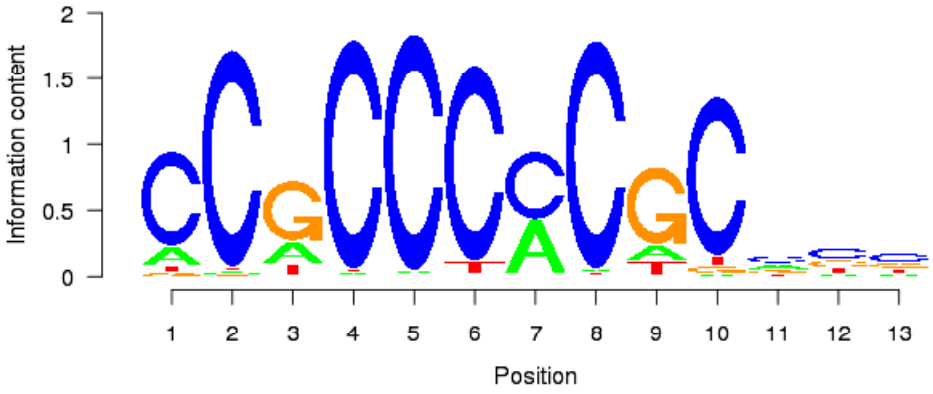

b

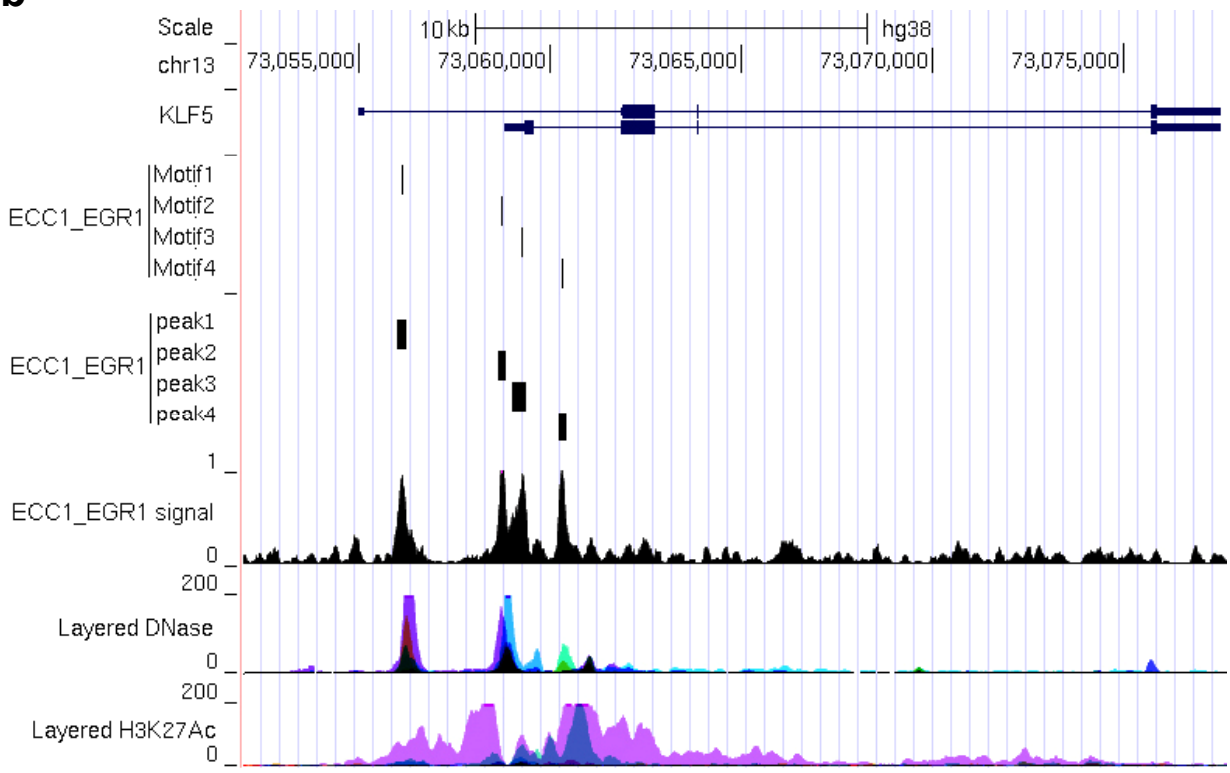

Supplementary Figure 16 | Annotation of the predicted EGR1 binding sites in the KLF5 gene using the Cistrome data browser. (**a**) Sequence logo of the EGR1 binding motif visualized using Cistrome. (**b**) The KLF5 upstream genomic region (chr13:73054976-73077542:GRCh38/hg38) is illustrated using the UCSC genome browser. ChIP-seq signals and peaks of H3K27ac, and DNAse-seq peaks were extracted from the Cistrome data. The read density of ChIP-seq signals is indicated in the Y-axis. ChIP-seq peaks of EGR1 in human cell line ECC1 from the Cistrome data and 4 predicted EGR1 binding motifs are indicated.

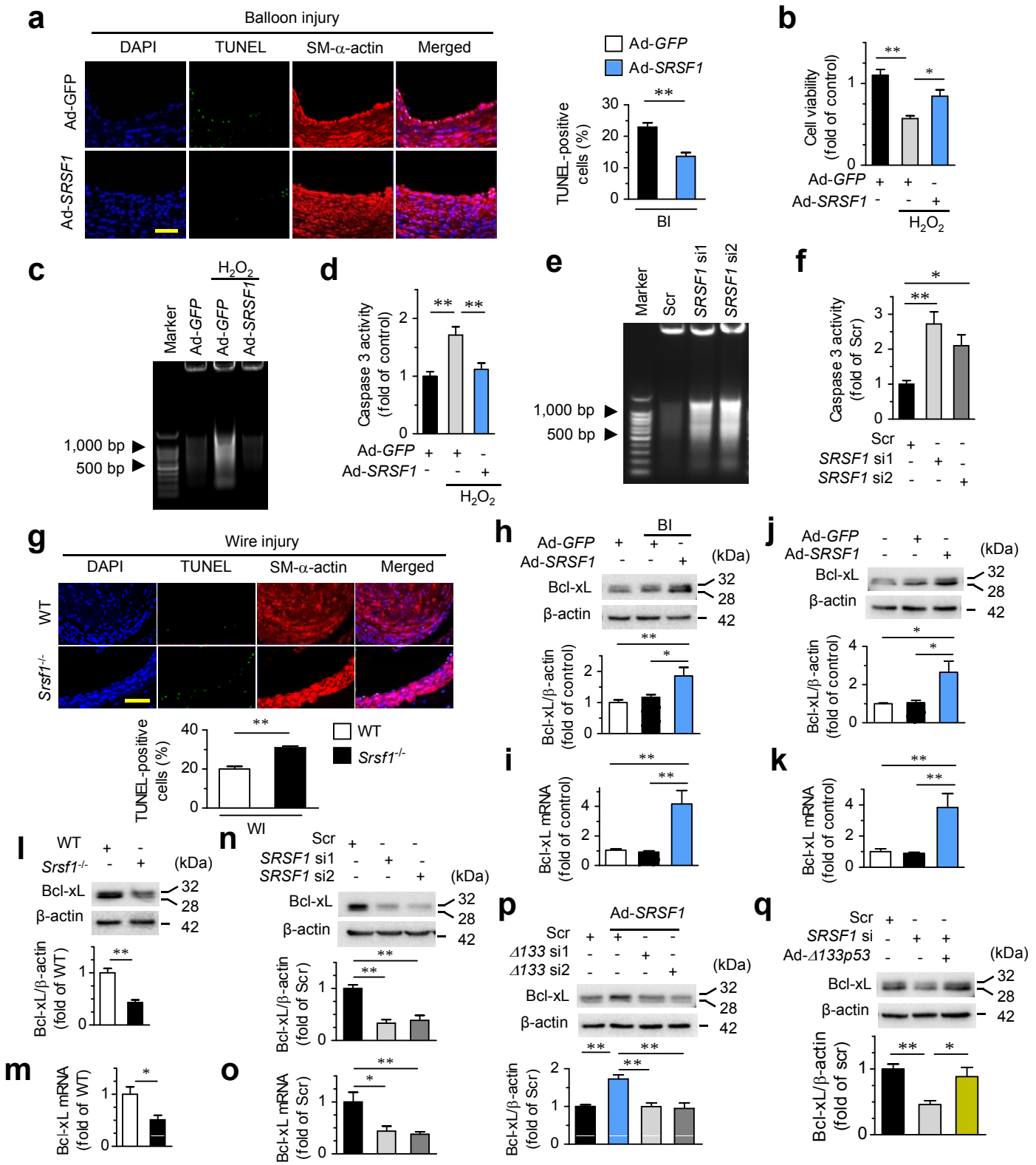

Supplementary Figure 17 | SRSF1 blockade of apoptosis contributes to neointima formation induced by wire-injury. (**a**) Representative photomicrographs (**left**) and averaged data (**right**) for TUNEL staining of rat carotid arteries transfected with Ad-*GFP* or Ad-SRSF1, two weeks after balloon injury; Green, TUNEL-positive VSMC nuclei; blue, DAPI-stained nuclei; red, VSMCs labeled with antibody to SM-α-actin; scale bar, 50 μm. *n* = 9 per group. (**b**,**c**,**d**) Cell viability (**b**), DNA laddering (**c**), and caspase 3 activity (**d**) in HASMCs treated with H_2O_2 (400 μM, 6 h) with or without Ad-*SRSF1* overexpression; *n* = 5 (**c**) or 9 samples (**b**,**d**). (**e**,**f**) DNA laddering (**e**) and caspase 3

activity (**f**) in HASMCs infected with *SRSF1* siRNAs; *n* = 5 (**e**) or 9 samples (**f**). (**g**) Representative photomicrographs and averaged data for TUNEL staining of carotid artery sections from WT and *Srsf1*$^{-/-}$ mice subjected to wire injury (4 weeks); Green, TUNEL-positive VSMC nuclei; blue, DAPI-stained nuclei; red, VSMCs labeled with antibody to SM-α-actinin; scale bar, 50 μm; *n* = 9 per group. (**h**) Representative western blots and averaged data showing Bcl-xL levels in rat carotid arteries transfected with Ad-*GFP* or Ad-*SRSF1* 4 days after balloon injury; *n* = 6 per group. (**i**) Real-time PCR data showing the Bcl-xL mRNA in rat carotid arteries transfected with Ad-*GFP* or Ad-*SRSF1*, one week after balloon injury; *n* = 8 per group. (**j**) Representative western blots and averaged data showing Bcl-xL levels in HASMCs with SRSF1 overexpression; *n* = 6 per group. (**k**) Real-time PCR data showing the Bcl-xL levels in HASMCs infected with Ad-*GFP* or Ad-*SRSF1*; *n* = 8 per group. (**l**) Representative western blots and averaged data showing Bcl-xL levels in arteries from *Srsf1*$^{-/-}$ and WT control mice; *n* = 7 per group. (**m**) Real-time PCR data showing the Bcl-xL levels in aortas from WT and *Srsf1*$^{-/-}$ mice; *n* = 8 per group. (**n**) Representative western blots and averaged data showing KLF5 levels in HASMCs with SRSF1-knockdown by *SRSF1* siRNAs; *n* = 5 per group. (**o**) Real-time PCR data showing the Bcl-xL levels in HASMCs infected with scrambled or *SRSF1* siRNAs; *n* = 8 per group. (**p**) Representative western blots and averaged data showing the Bcl-xL levels in HASMCs infected with scrambled or *Δ133p53* siRNAs (*Δ133* si1 and *Δ133* si2) with or without of Ad-*SRSF1* overexpression; *n* = 9 per group. (**q**) Representative western blots and averaged data showing the Bcl-xL levels in HASMCs infected with scrambled or *SRSF1* siRNA1 (*SRSF1* si) with or without overexpression of Ad-*Δ133p53*; *n* = 7 per group. Scr indicates scrambled siRNA control. BI, balloon injury. WI, wire injury. **P* <0.05, ***P* <0.01, Student's *t*-test (**a**,**g**,**l**,**m**) or one-way ANOVA (**b**,**d**,**f**,**h-k**,**n**-**q**). Data are mean ± s.e.m. of three (**m**) or four (**a**-**g**,**o**) or five (**h-l**,**n**-**q**) independent experiments.

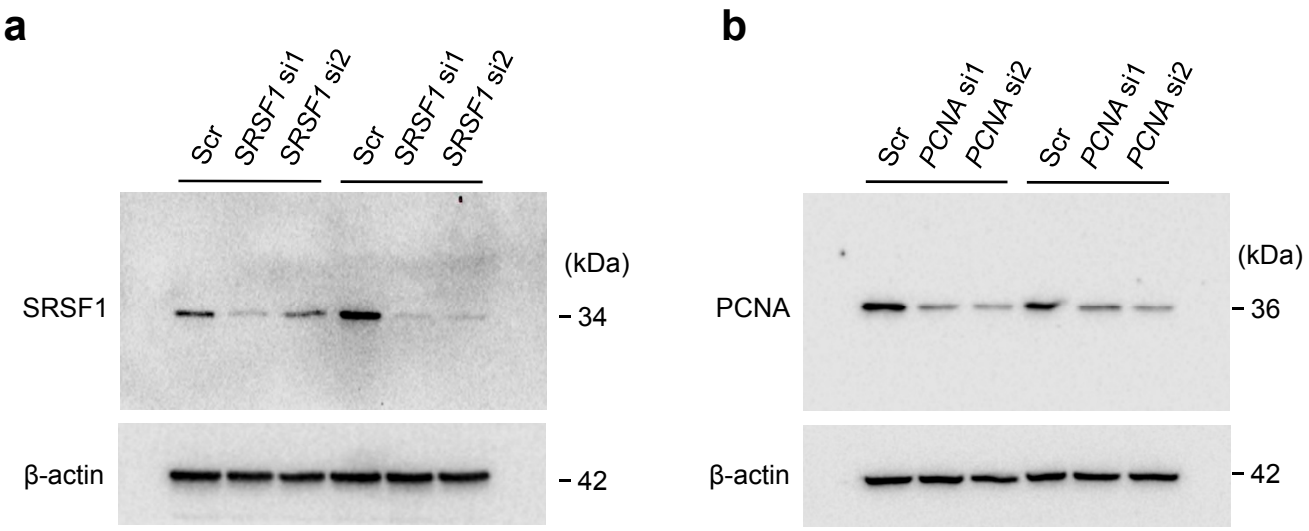

Supplementary Figure 18 | Knock down of SRSF1 or PCNA in HASMCs. (**a**) Representative western blots showing SRSF1 levels in HASMCs with SRSF1-knockdown by *SRSF1* siRNAs. Antibody for SRSF1 from Invitrogen (catalog number 32-4500), recognizes the first 97 amino acids of SRSF1. (**b**) Representative western blots showing PCNA levels in HASMCs with PCNA-knockdown by *PCNA* siRNAs. Antibody for PCNA from Signaling Technology (catalog number 2586), recognizes the protein region within the amino acid residues 111-125.

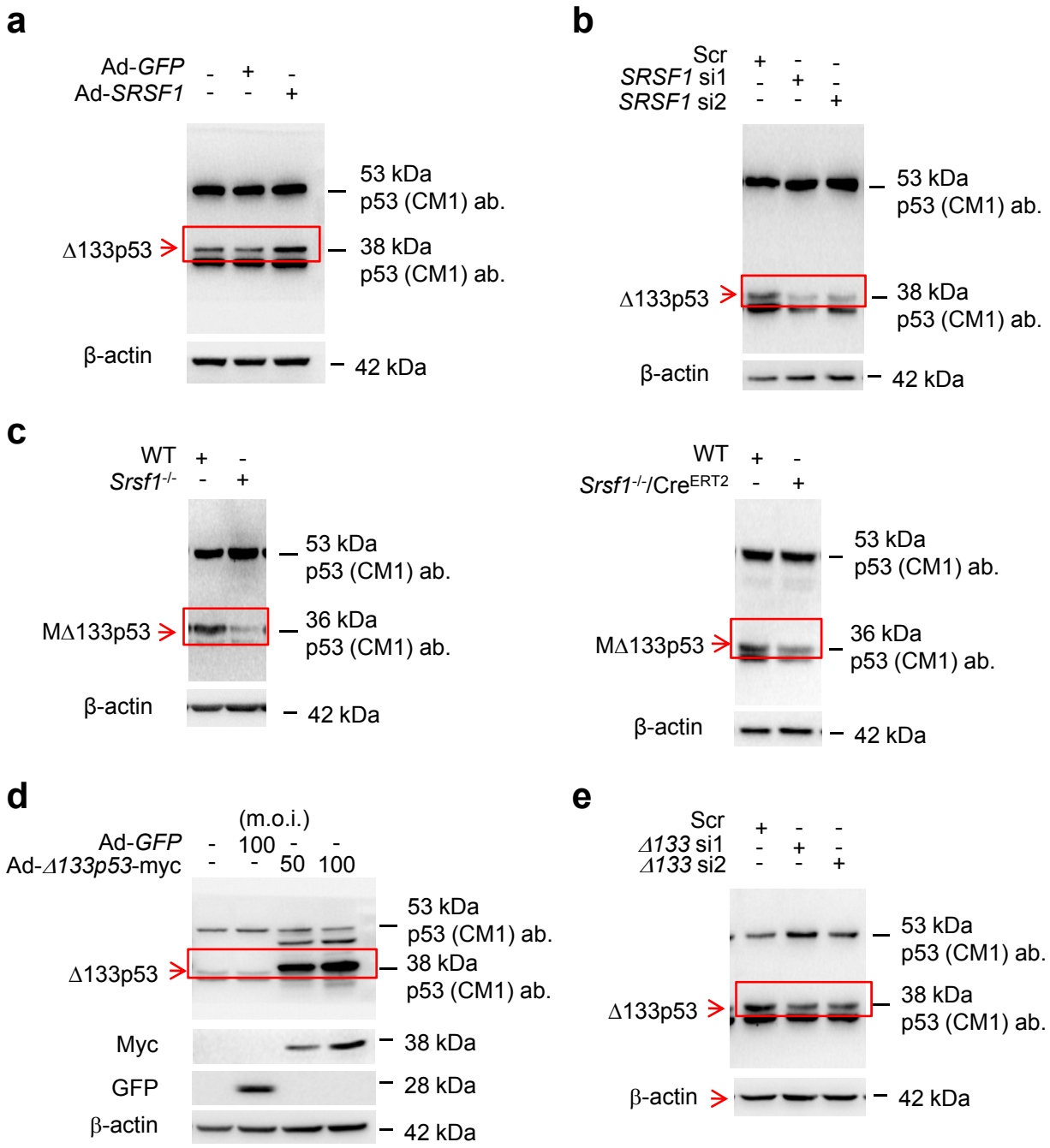

Supplementary Figure 19 | Representative full-length gels showing all p53 isoforms. (**a**,**b**) Gels for p53 isoforms in HASMCs with SRSF1-overexpression (**a**) and SRSF1-knockdown by *SRSF1* siRNAs (*SRSF1* si1 and *SRSF1* si2) (**b**). (**c**) Gels for p53 isoforms in vessels from *Srsf1*$^{-/-}$ and WT control mice at 56 days after birth. (**d**,**e**) Gels for p53 isoforms in HASMCs with Δ133p53-overexpression (**d**) or Δ133p53-knockdown by *Δ133p53* siRNAs (*Δ133* si1 and *Δ133* si2) (**e**). The antibody we used to detect Δ133p53 (and Δ157p53) was p53 (CM1) antibody (Vector Laboratories, VP-P955), a rabbit polyclonal antibody raised against recombinant full-length human p53 protein that recognizes all p53 isoforms.

Supplementary Figure 20 | Uncropped images of blots in Figure 1-9 and Supplementary Figure 1-19.

Fig. 1d

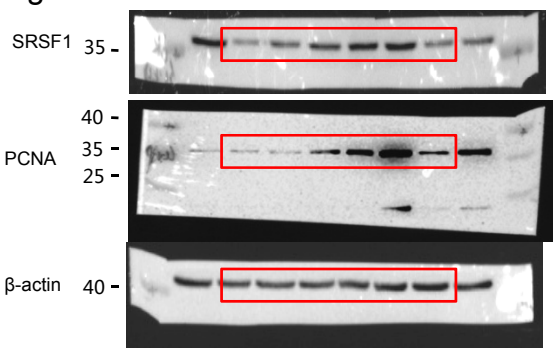

Fig. 2a

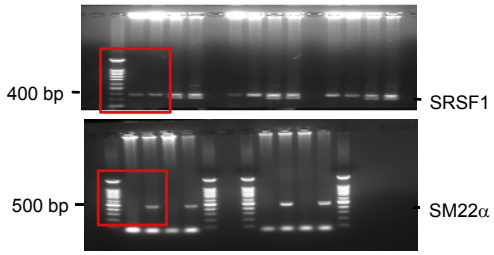

Fig. 2b

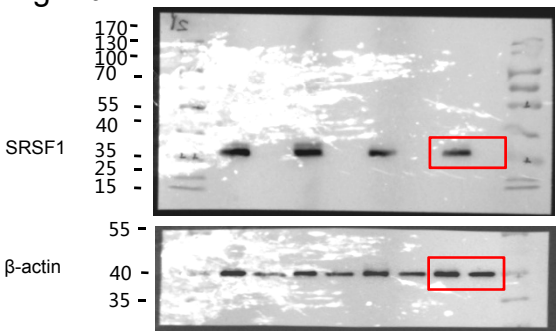

Fig. 3a

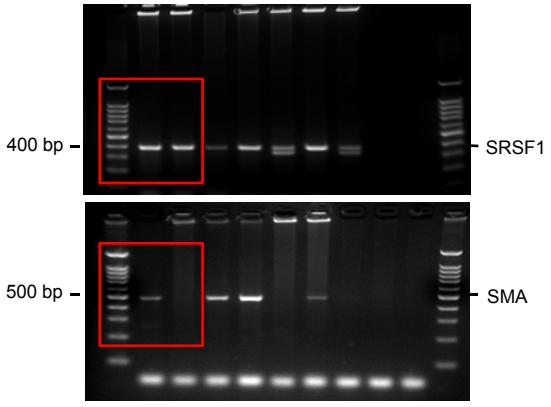

Fig. 3b

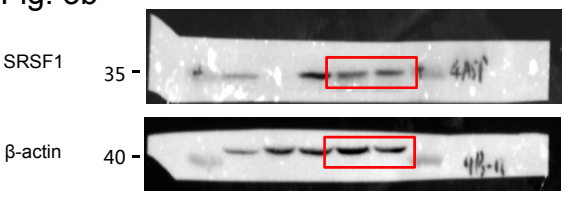

Fig. 1f

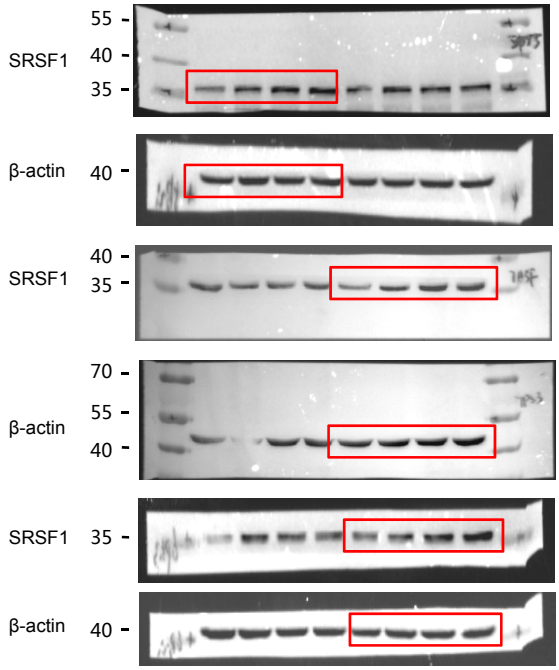

Fig. 4a

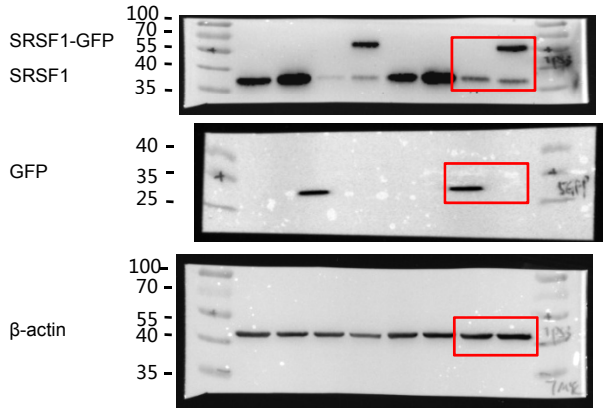

Fig. 4e

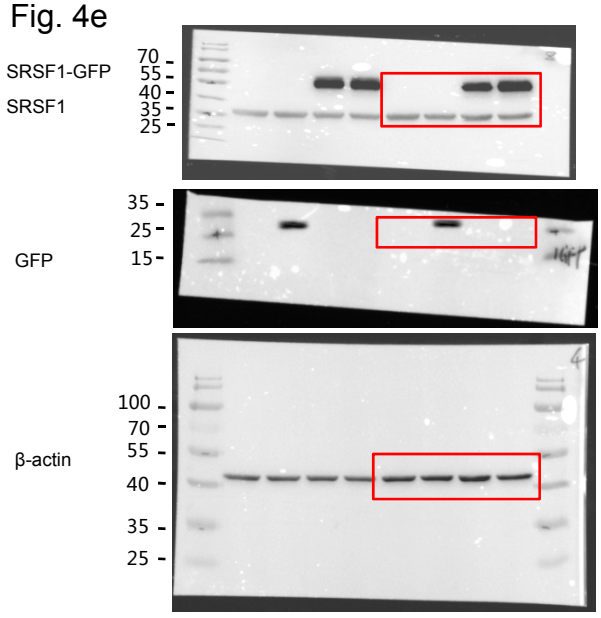

Fig. 4j

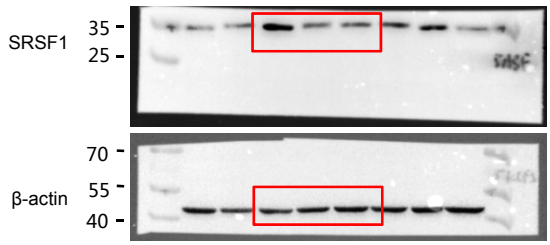

Fig. 5e

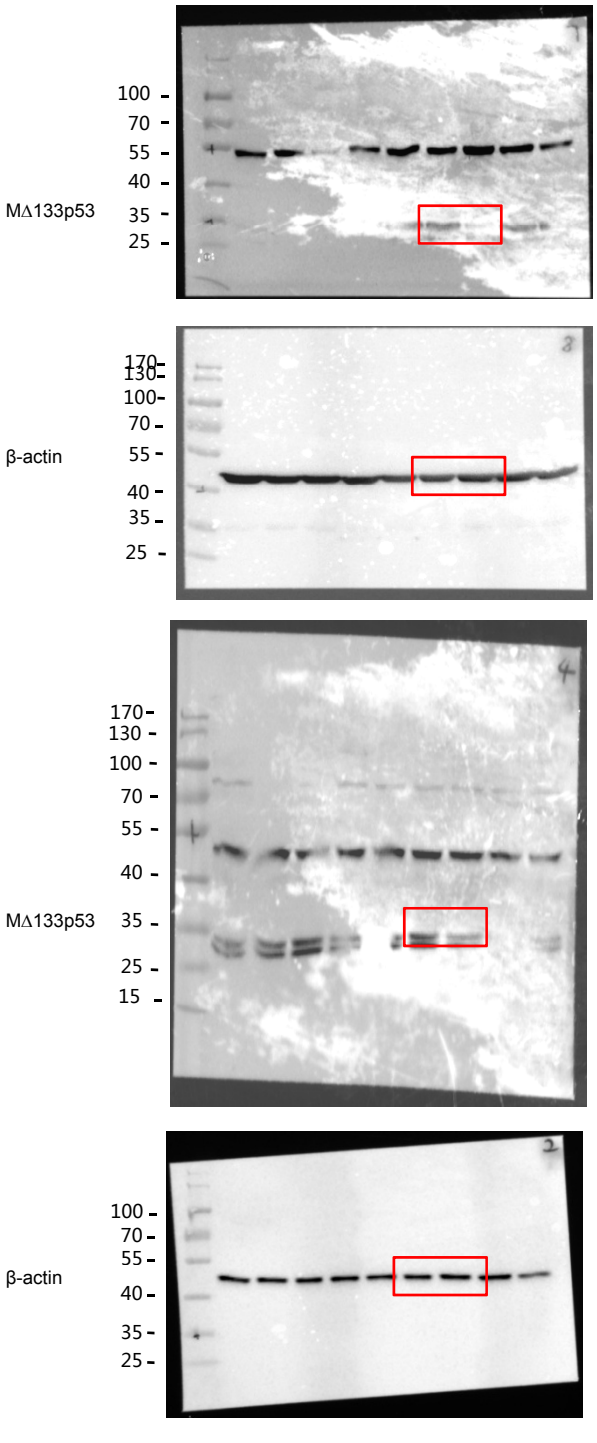

Fig. 4f

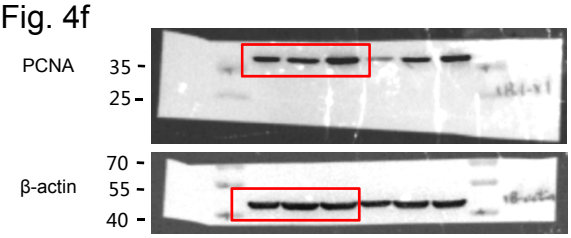

Fig. 4k

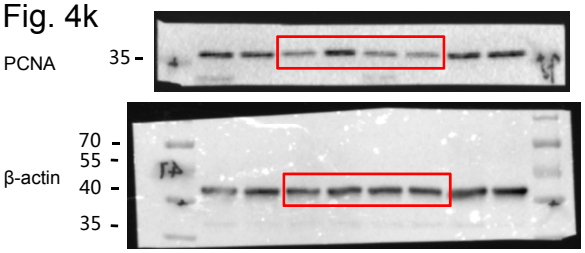

Fig. 5b

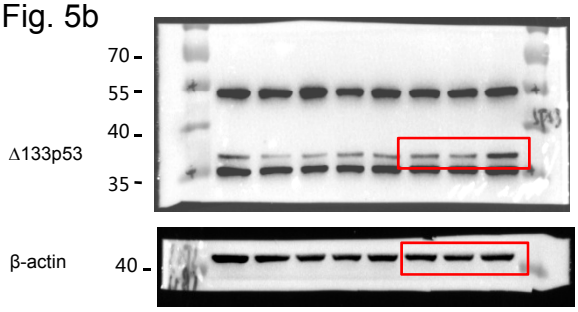

Fig. 5d

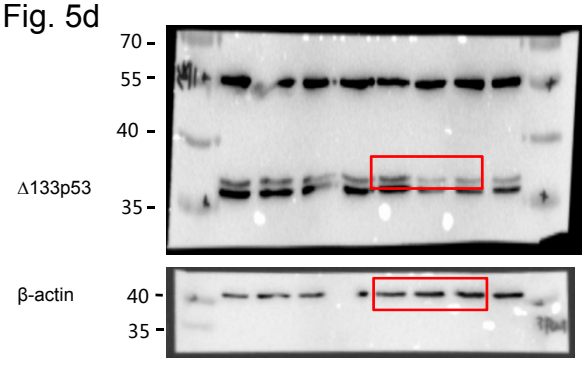

Fig. 5f

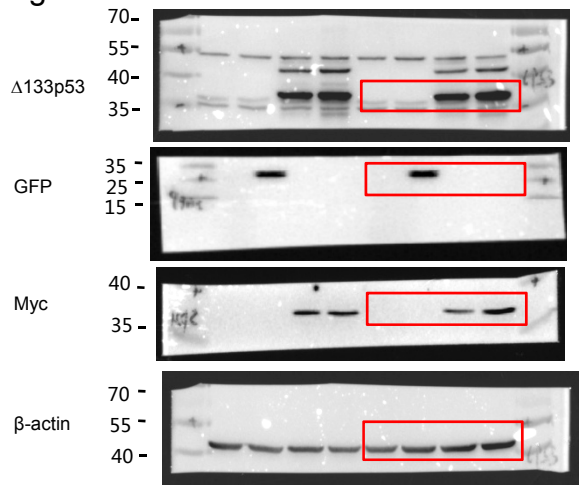

Fig. 5g

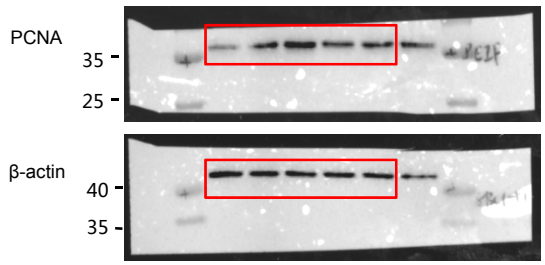

Fig. 5n

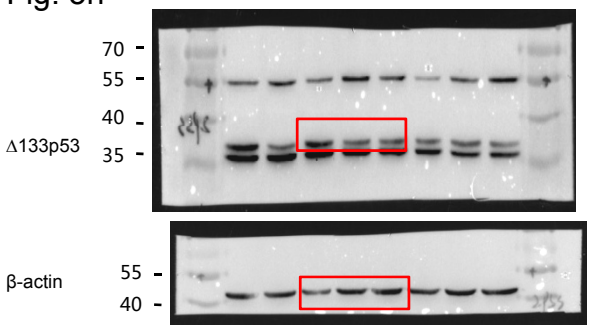

Fig. 5o

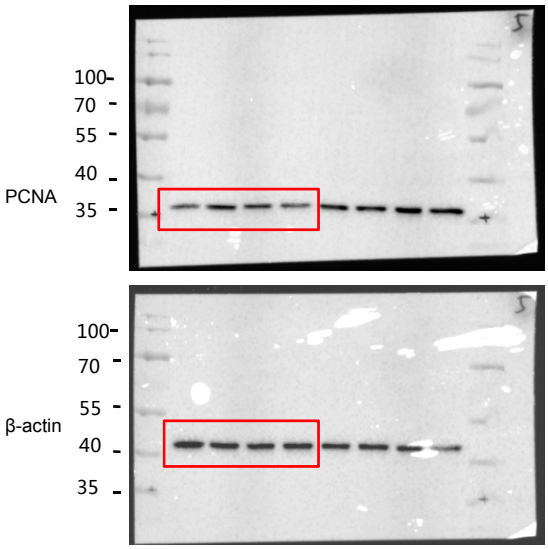

Fig. 5r

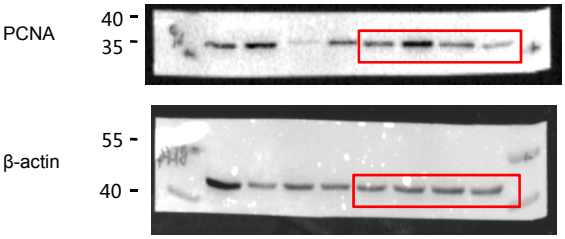

Fig. 6e

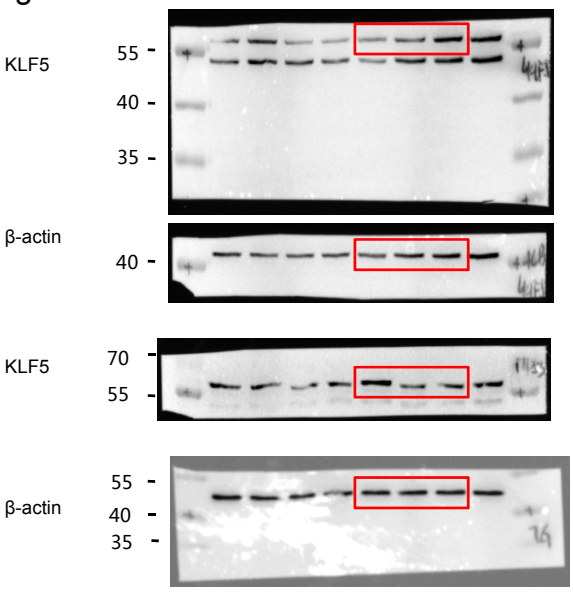

Fig. 6c

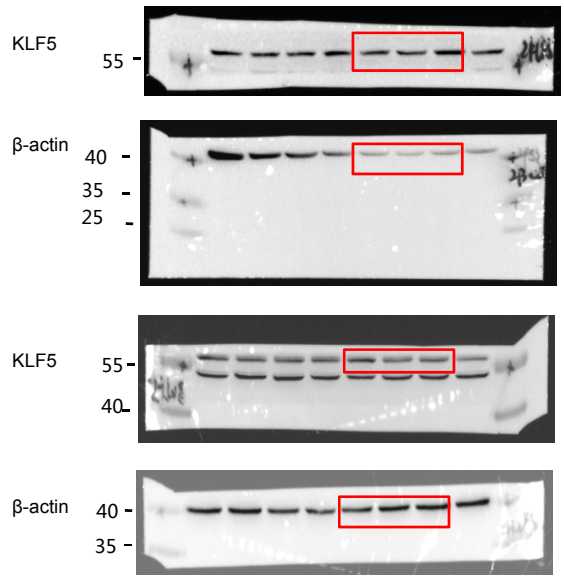

Fig. 6g

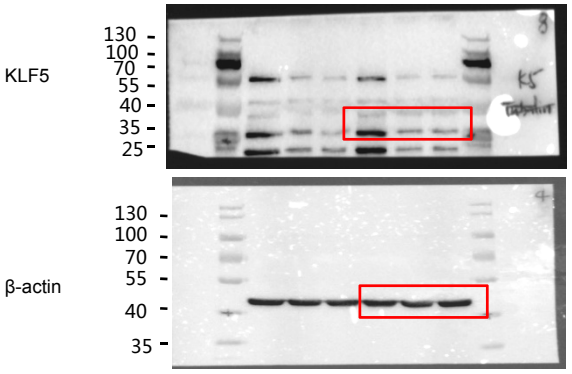

Fig. 6h

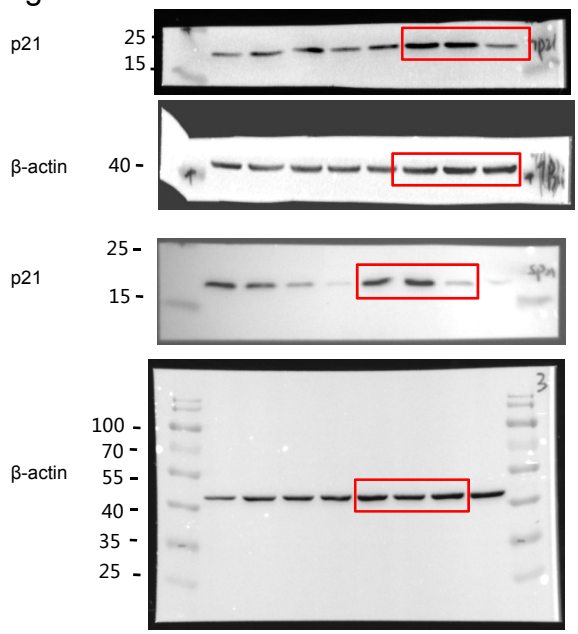

Fig. 6i

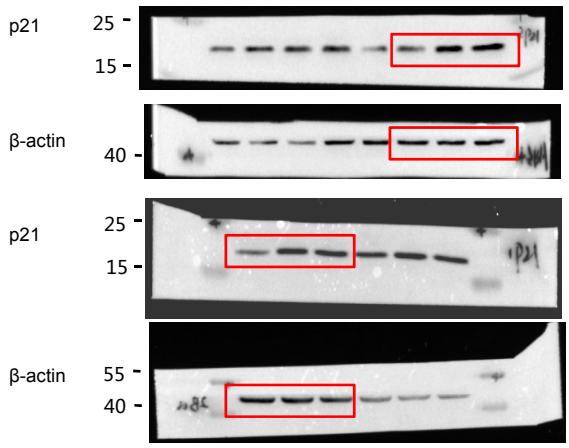

Fig. 6j

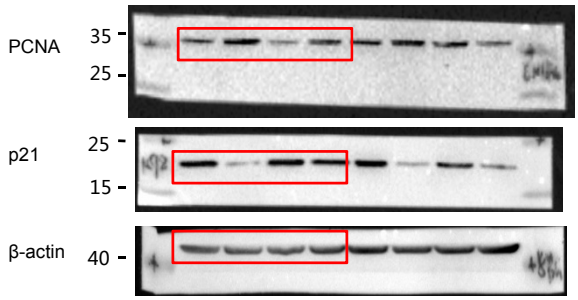

Fig. 6k

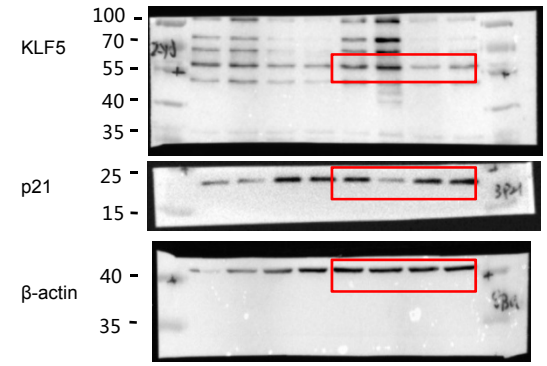

Fig. 6l

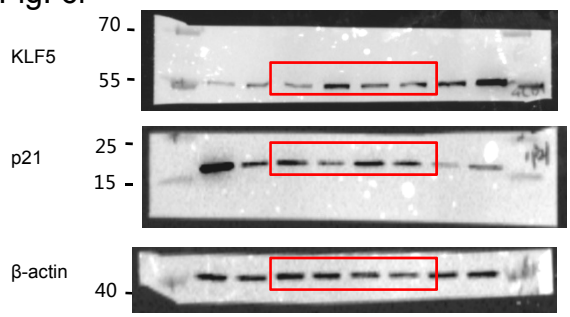

Fig. 6m

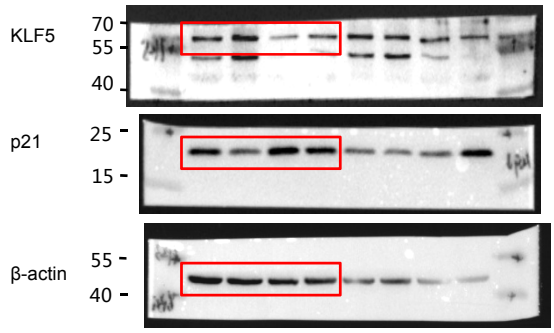

Fig. 6n

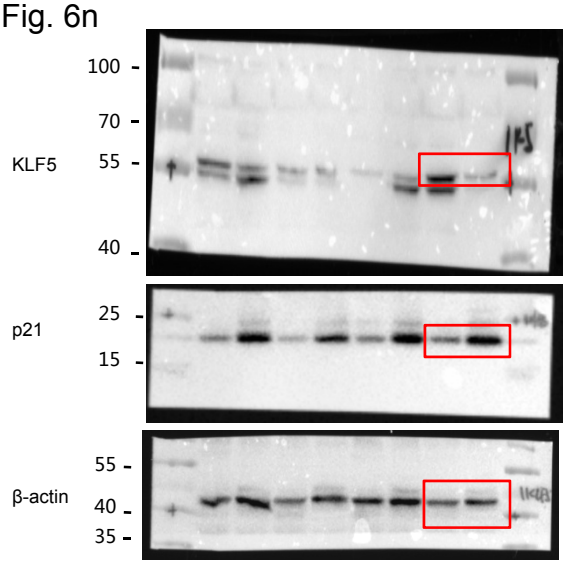

Fig. 6o

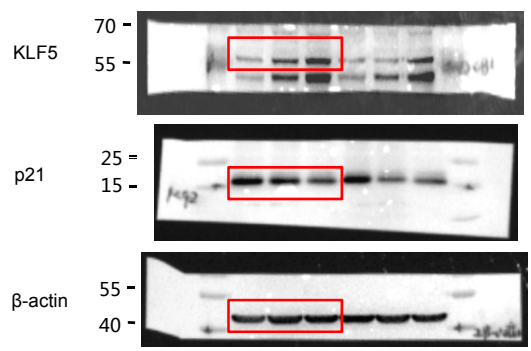

Fig. 7a

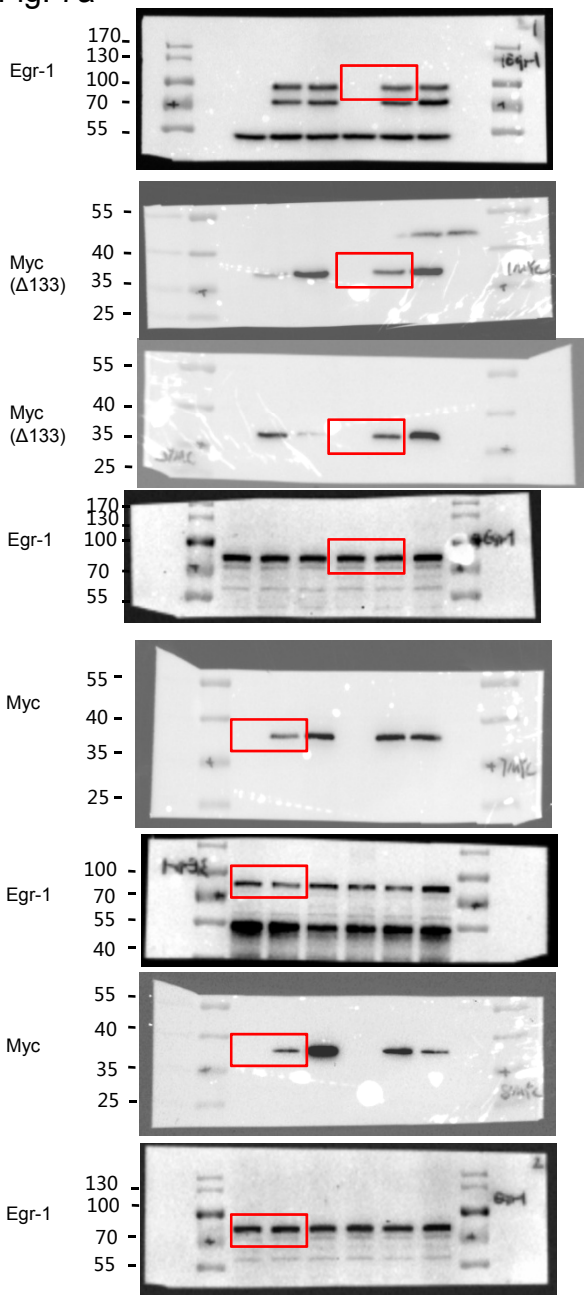

Fig. 7e

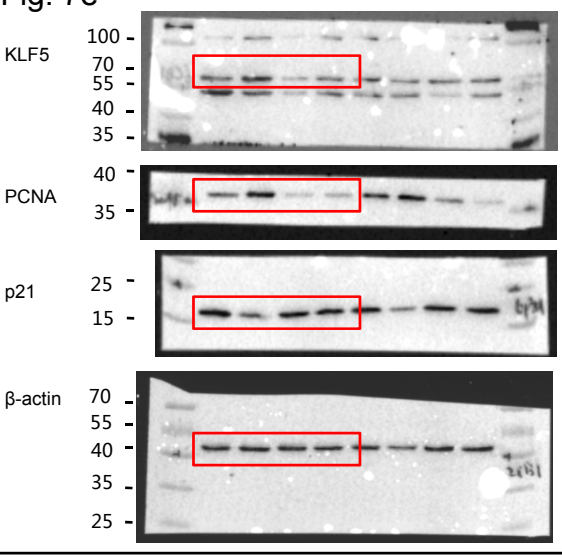

Fig. 7c

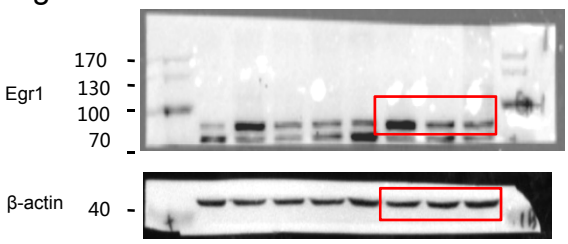

Fig. 7f

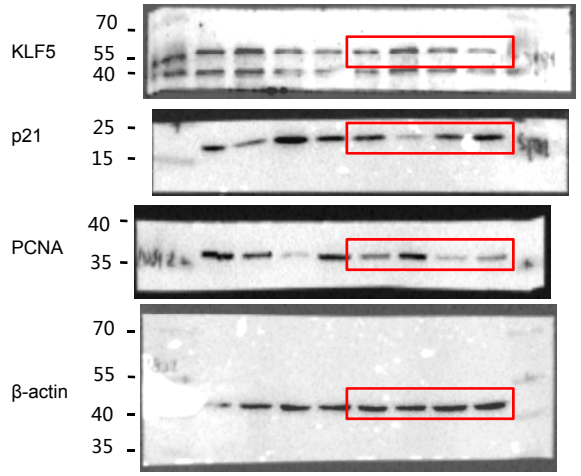

Fig. 8c

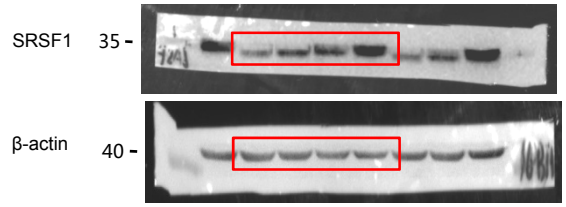

Fig. 8d

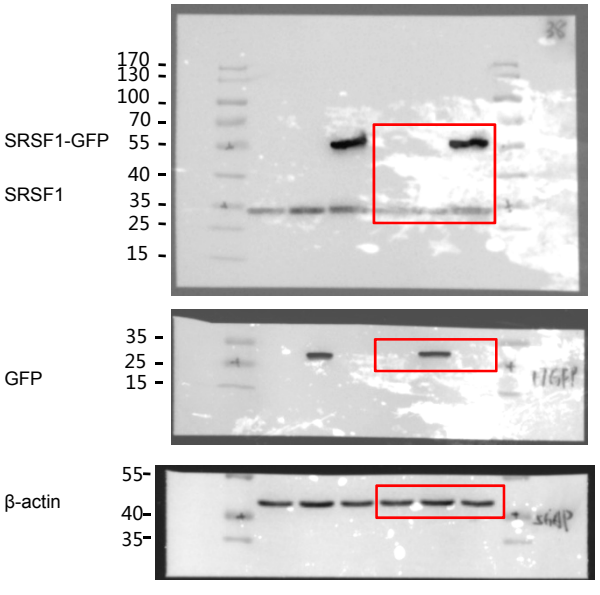

Fig. 8e

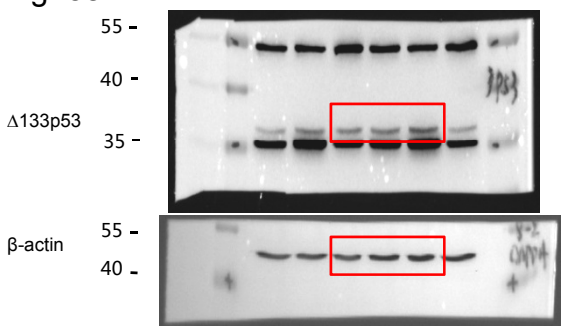

Fig. 8f

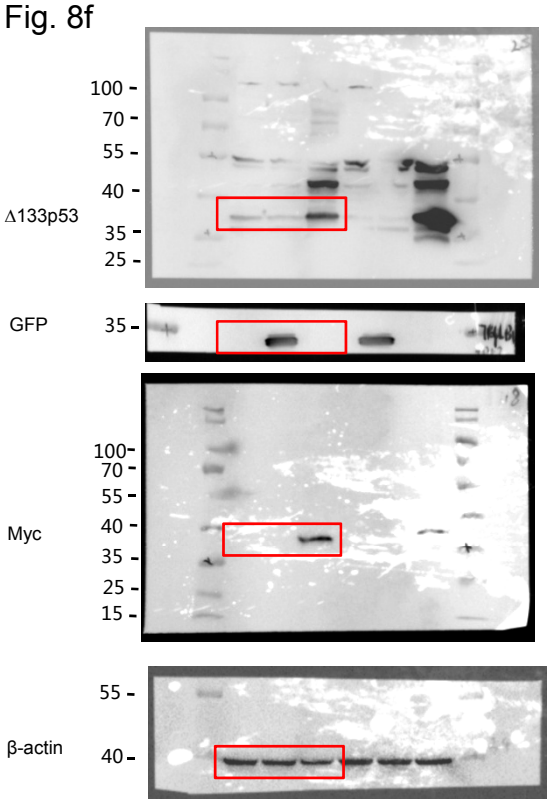

Fig. 8m

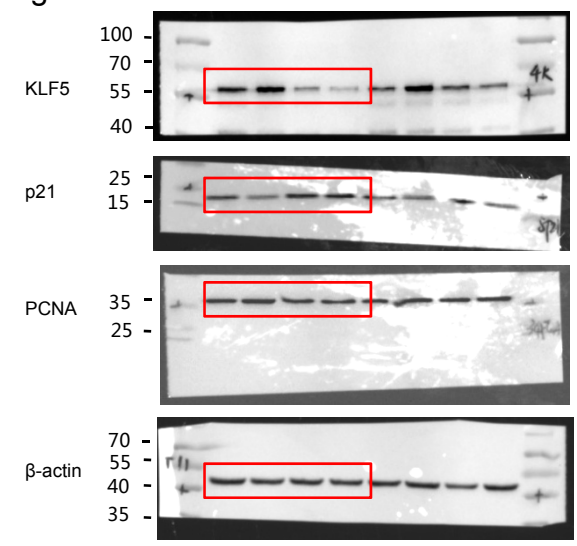

Fig. 8h

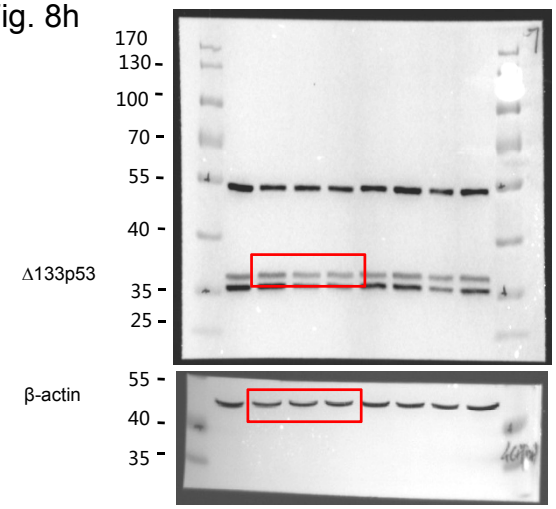

Fig. 8j

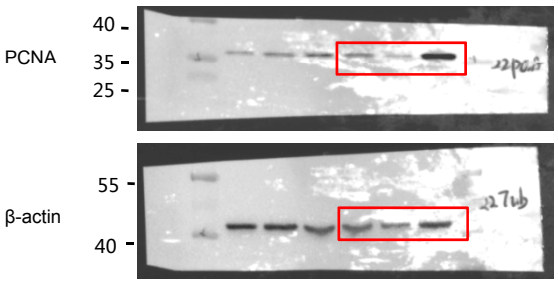

Fig. 8k

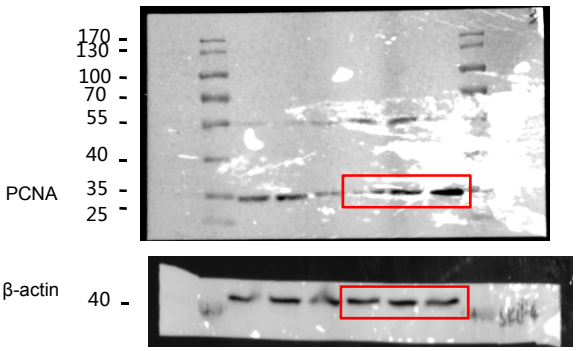

Fig. 9b

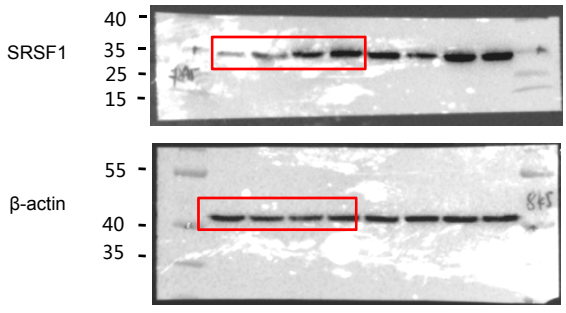

Fig. 9c

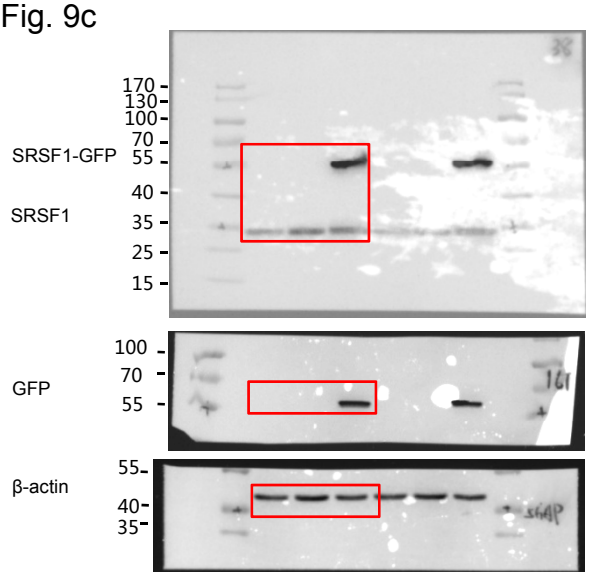

Fig. 9d

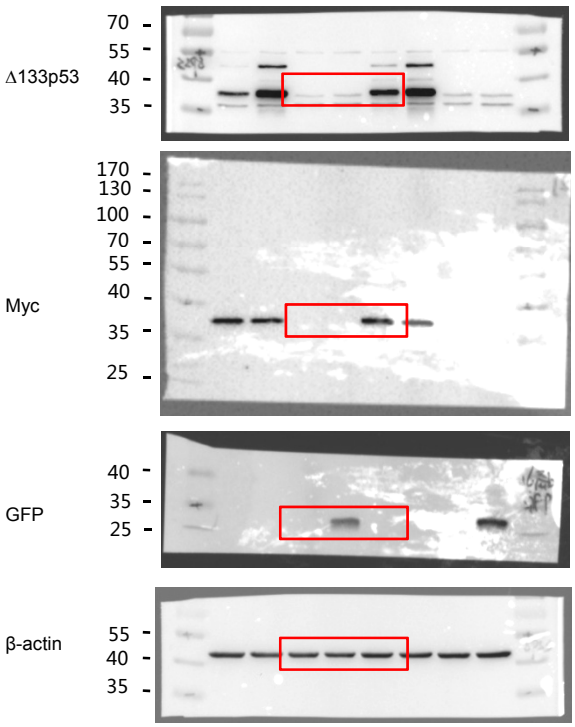

Fig. 9e

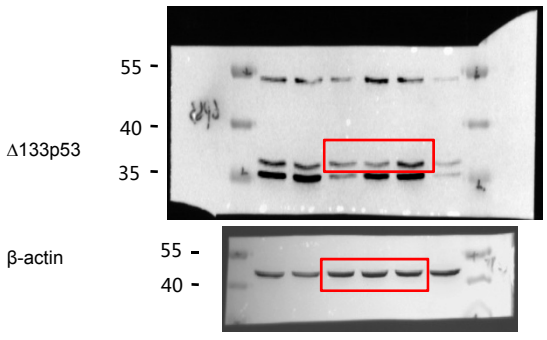

Fig. 9g

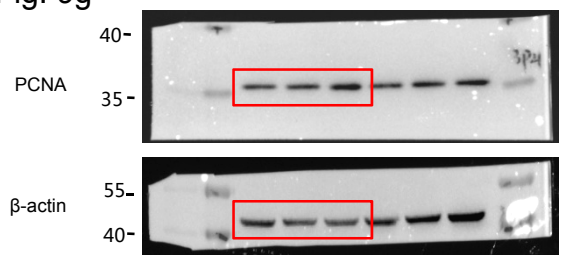

Fig. 9h

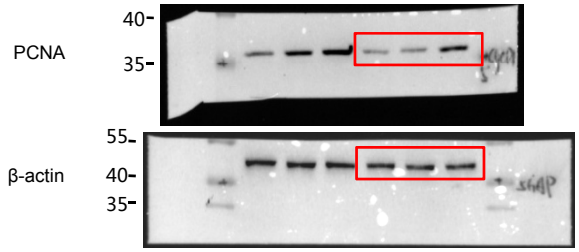

Fig. 9j

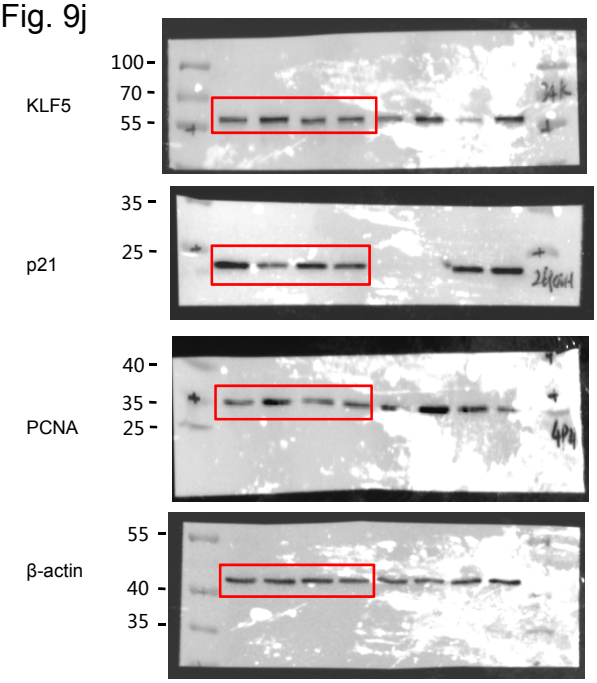

Fig. 9k

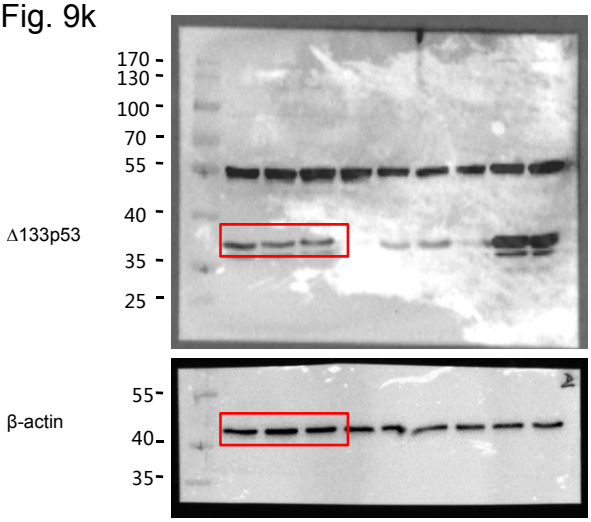

Supplementary Fig. 1b

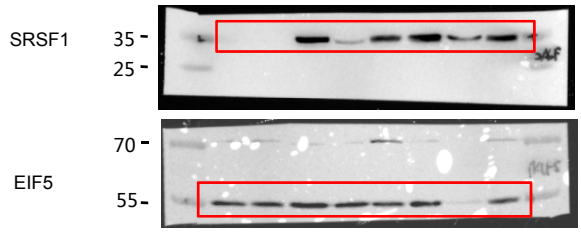

Supplementary Fig. 1c

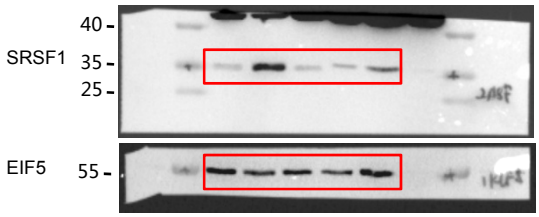

Supplementary Fig. 7b

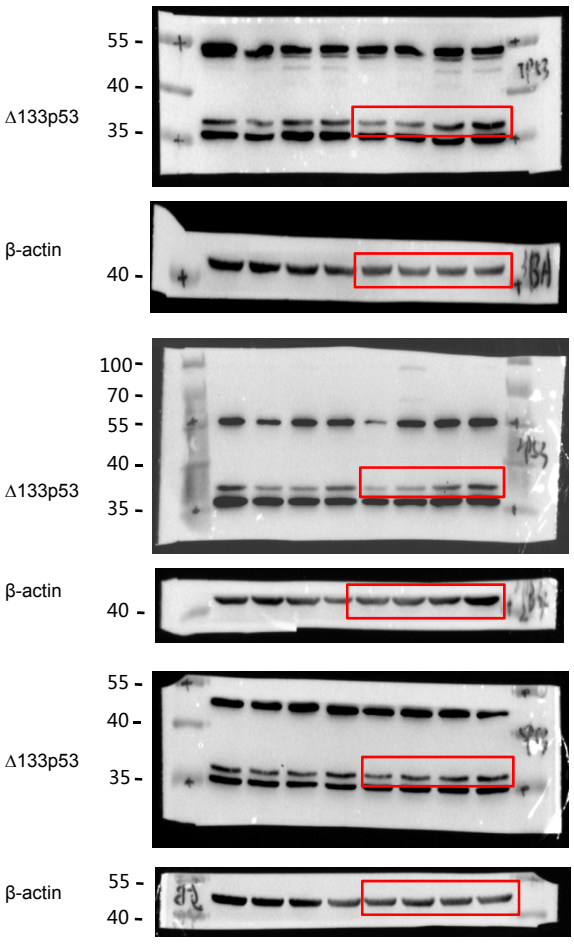

Supplementary Fig. 2c

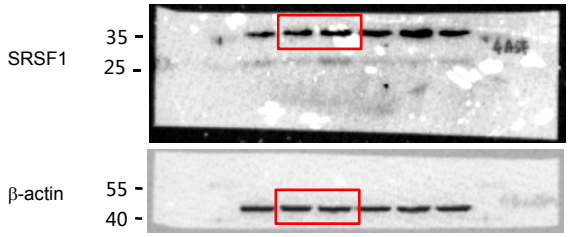

Supplementary Fig. 3a

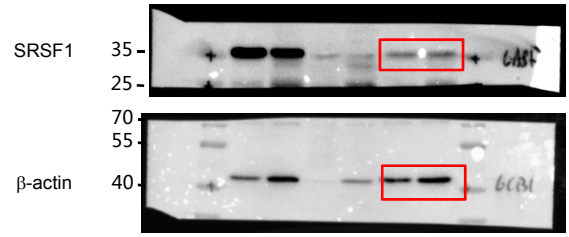

Supplementary Fig. 5

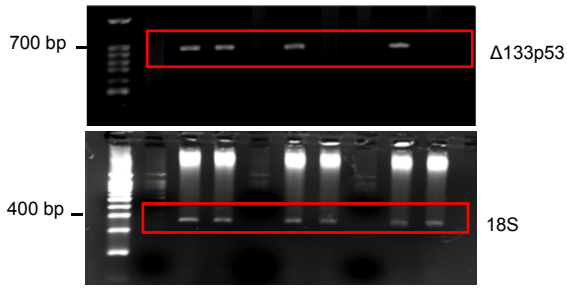

Supplementary Fig. 8a

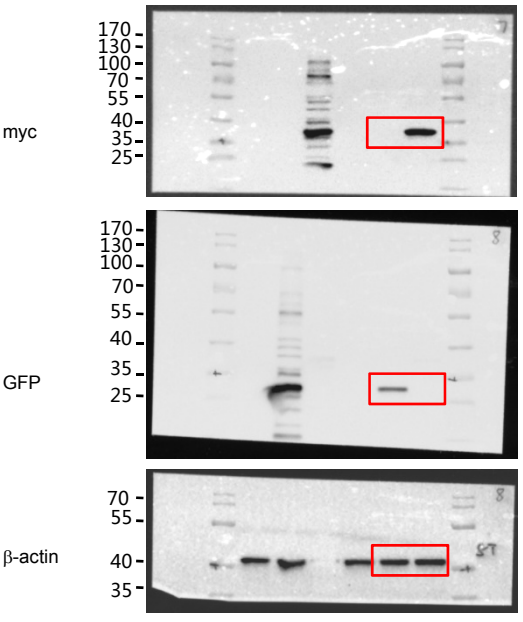

Supplementary Fig. 8b

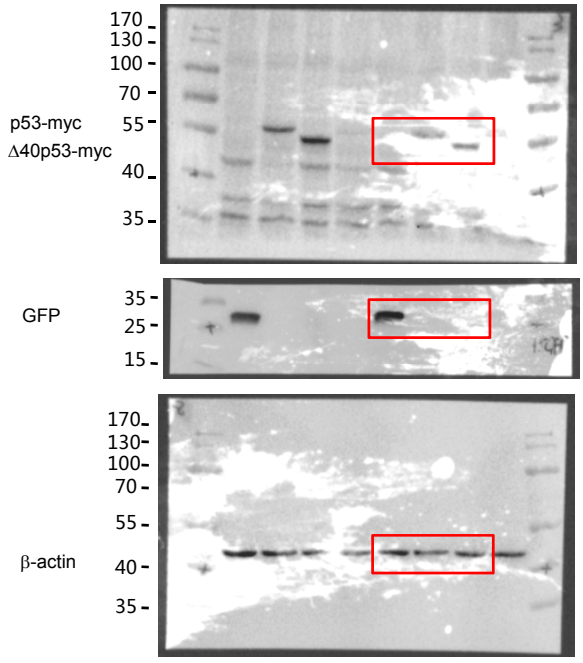

Supplementary Fig. 8d

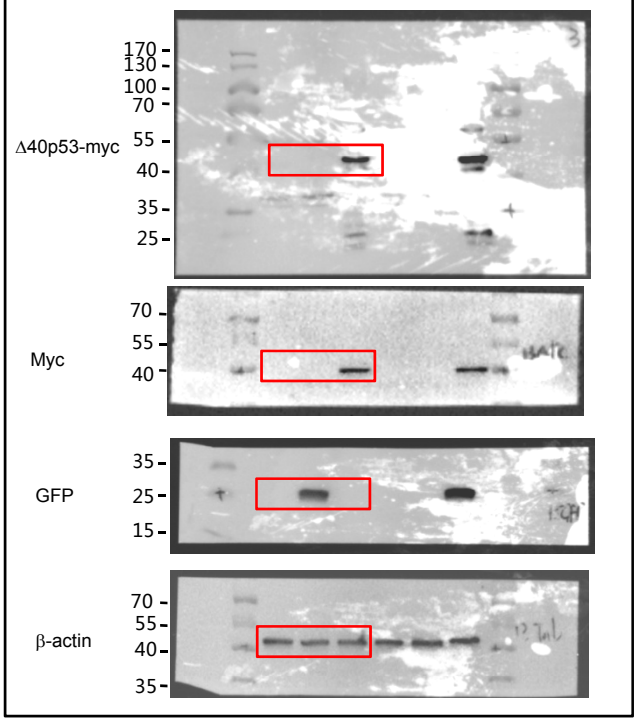

Supplementary Fig. 8c

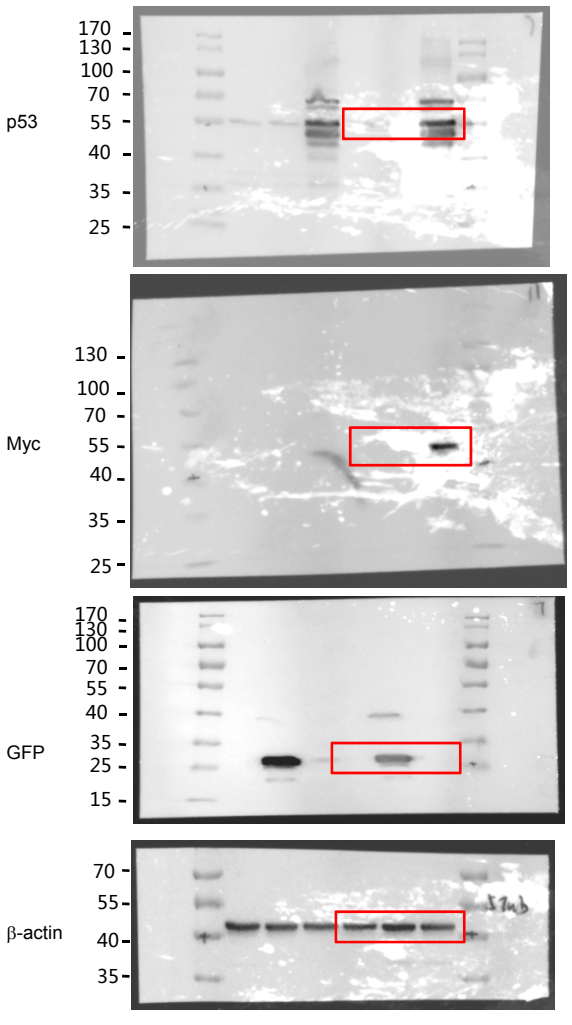

Supplementary Fig. 9b

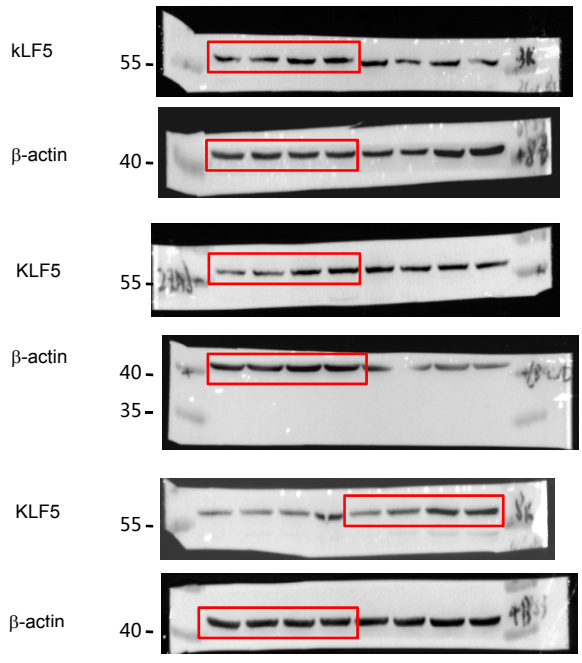

Supplementary Fig. 10a

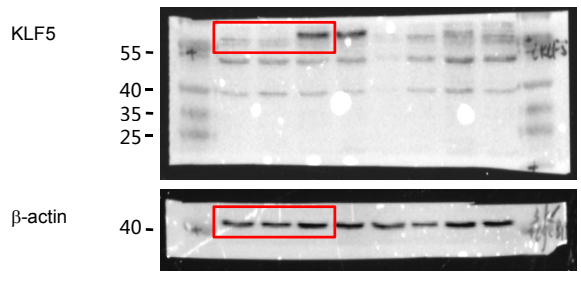

Supplementary Fig. 10b

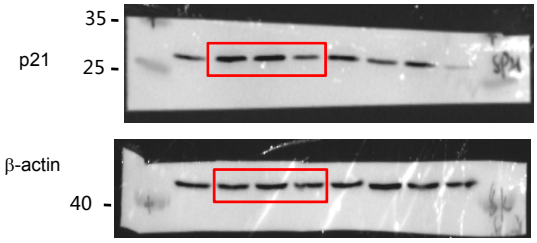

Supplementary Fig 17c

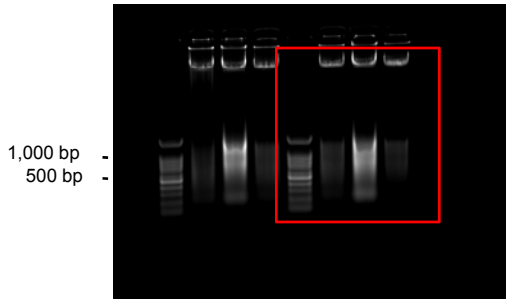

Supplementary Fig 17e

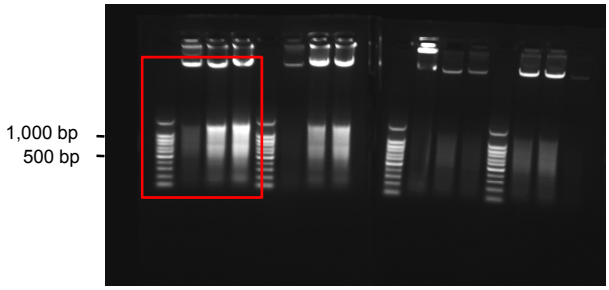

Supplementary Fig. 17h

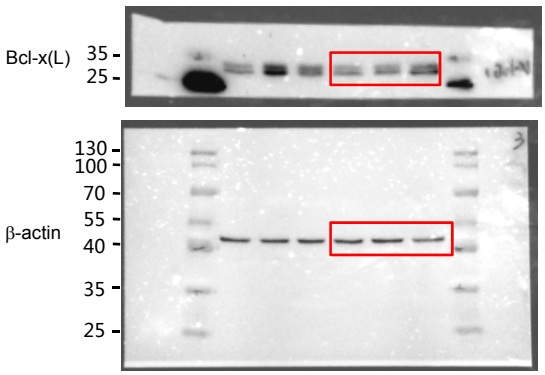

Supplementary Fig. 17j

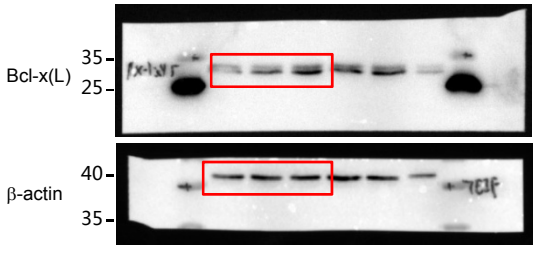

Supplementary Fig. 15

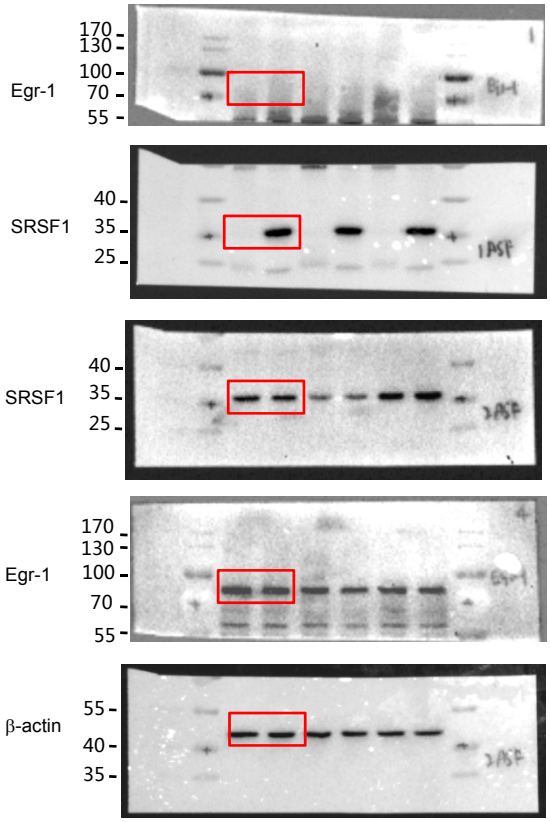

Supplementary Fig. 17l

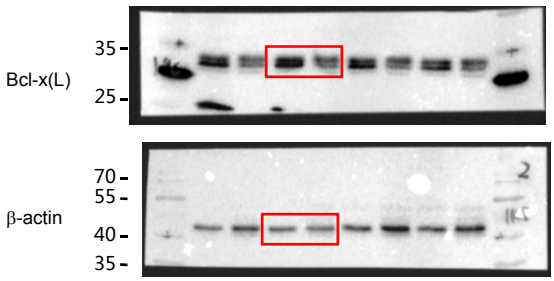

Supplementary Fig. 17n

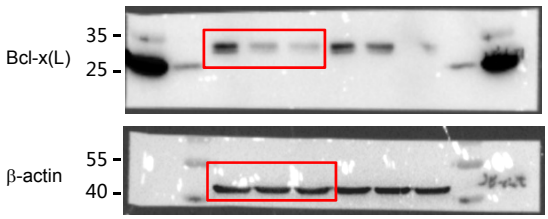

Supplementary Fig. 17p

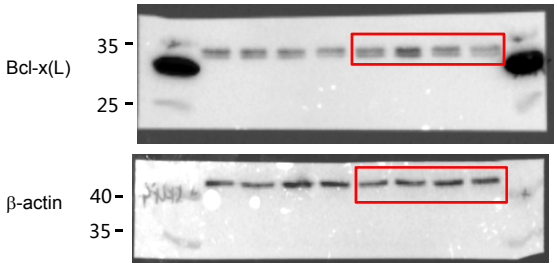

Supplementary Fig. 17q

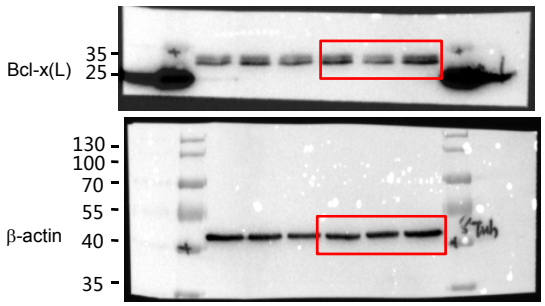

Supplementary Fig. 19a

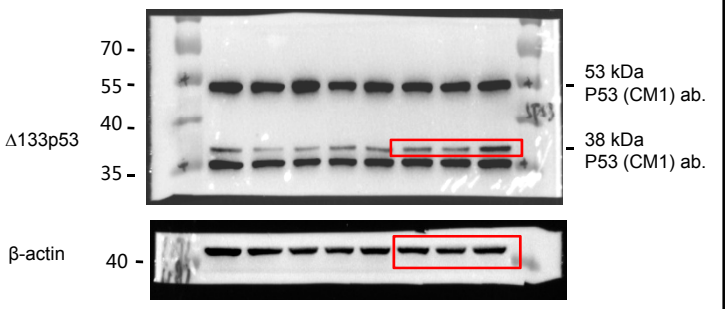

Supplementary Fig. 18a

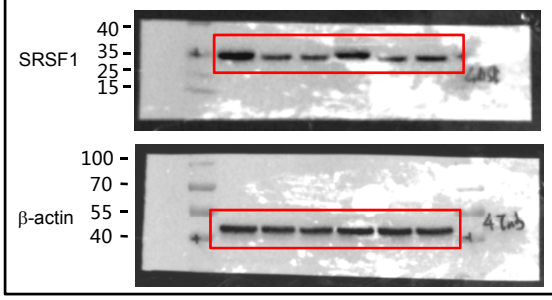

Supplementary Fig. 18b

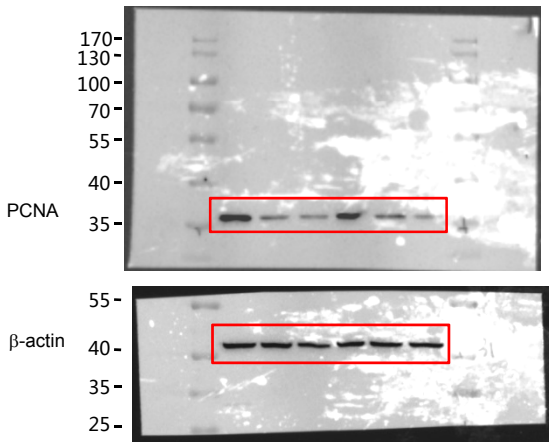

Supplementary Fig. 19c

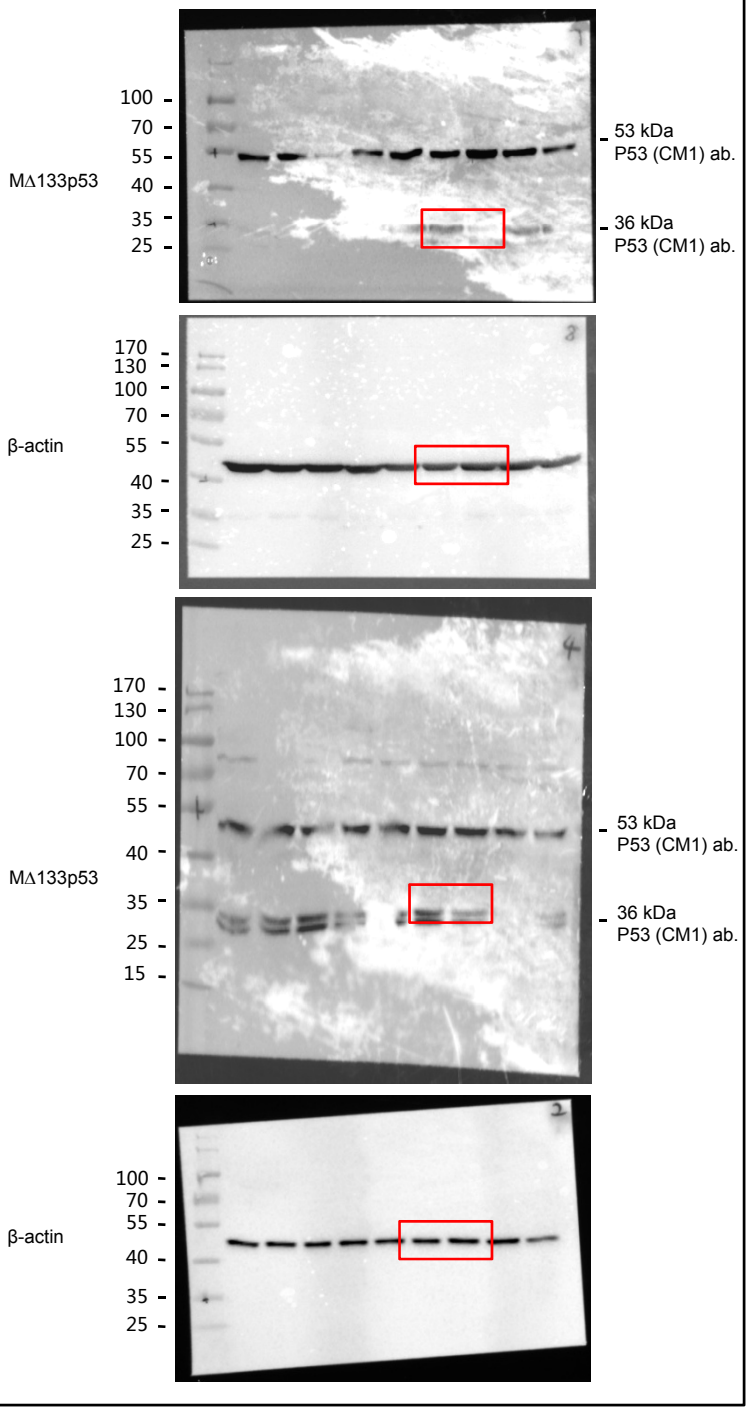

Supplementary Fig. 19b

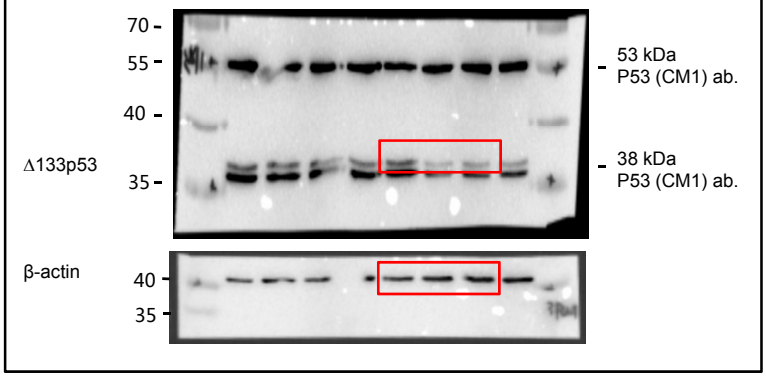

Supplementary Fig. 19d

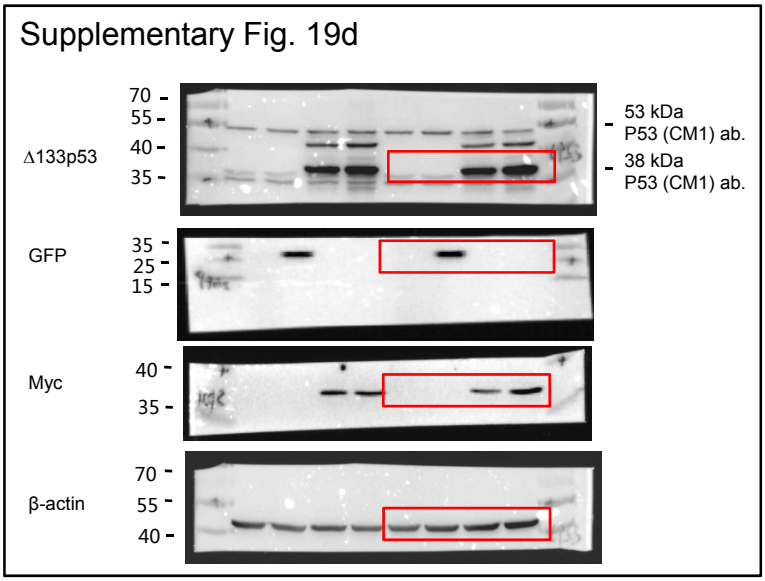

Supplementary Fig. 19e

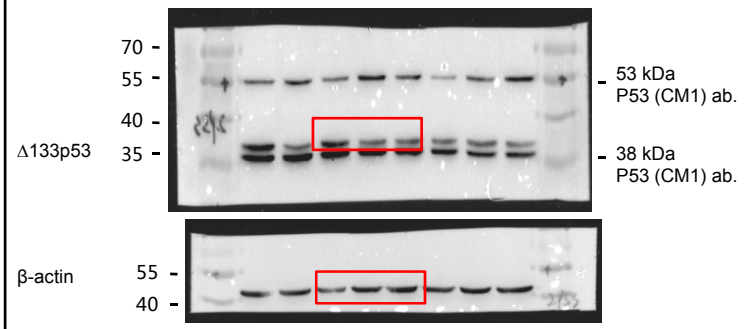

Supplementary Table 1

Gene expression profiling of human aortic smooth muscle cells transfected with Ad-*Δ133p53* and Ad-*GFP*, or treated with Ang II.

Gene title	Gene symbol	Fold of change (Δ133p53/GFP)	Fold of change (Ang II/GFP)
Adrenomedullin 2	ADM2	2.10	1.79
Rho GTPase activating protein 26	ARHGAP26	7.83	2.53
Rho/Rac guanine nucleotide exchange factor (GEF) 2	ARHGEF2	1.65	1.58
Rho guanine nucleotide exchange factor (GEF) 28	ARHGEF28	4.91	2.78
BMP and activin membrane-bound inhibitor homolog (Xenopus laevis)	BAMBI	3.04	2.46
Calmodulin 2 (phosphorylase kinase, delta)	CALM2	2.11	1.61
CAP, adenylate cyclase-associated protein, 2 (yeast)	CAP2	4.18	3.58
Dimethylarginine dimethylaminohydrolase 1	DDAH1	3.75	3.75
Deleted in liver cancer 1	DLC1	1.54	1.99
EPH receptor A5	EPHA5	1.50	2.57
Fms-related tyrosine kinase 1	FLT1	2.16	1.76
Guanine nucleotide binding protein (G protein), beta polypeptide 4	GNB4	1.87	1.61
Histone deacetylase 9	HDAC9	1.58	2.06
Inhibin, beta A	INHBA	8.38	5.40
Intersectin 1 (SH3 domain protein)	ITSN1	1.67	1.59
Kruppel-like factor 5 (intestinal)	KLF5	3.69	3.75
Met proto-oncogene (hepatocyte growth factor recepto	MET	2.68	1.59
Myosin, heavy chain 10, non-muscle	MYH10	1.95	4.03
Myosin, light chain 12A, regulatory, non-sarcomeric	MYL12A	2.16	2.43
Myosin, light chain 12B, regulatory	MYL12B	1.53	1.80
Myosin, light chain 9, regulatory	MYL9	1.65	1.73
Neural precursor cell expressed, developmentally down-regulated 4-like, E3 ubiquitin protein ligase	NEDD4L	1.67	1.58
Oxytocin receptor	OXTR	6.88	8.67
Phosphodiesterase 1C, calmodulin-dependent 70kDa	PDE1C	2.42	1.63
Phosphodiesterase 3A, cGMP-inhibited	PDE3A	1.55	1.58
Retinol dehydrogenase 10 (all-trans)	RDH10	2.01	6.47
Regulator of G-protein signaling 4	RGS4	6.28	1.82
Sodium channel, voltage-gated, type III, alpha subunit	SCN3A	1.87	2.87
Syndecan 2	SDC2	1.63	1.90
Sema domain, seven thrombospondin repeats (type 1	SEMA5A	1.45	3.12
Serpin peptidase inhibitor, clade E (nexin, plasminogen activator inhibitor type 1), member 1	SERPINE1	6.06	2.49
SMAD specific E3 ubiquitin protein ligase 2	SMURF2	1.87	1.53
Sphingosine kinase 1	SPHK1	2.52	2.04
Transforming growth factor, beta receptor 1	TGFBR1	2.18	1.94
Thrombospondin 1	THBS1	2.03	1.97
Tribbles homolog 3 (Drosophila)	TRIB3	6.69	2.46
Transient receptor potential cation channel, subfamily C, member 4	TRPC4	3.30	3.06
Transient receptor potential cation channel, subfamily C, member 6	TRPC6	3.21	3.30
Vascular endothelial growth factor C	VEGFC	1.50	1.50

Supplementary Table 2

Antibodies information

Antibodies name	Products information	Working concentration
SRSF1	Invitrogen, 32-4500; recognizes the first 97 amino acids of SRSF1	1:1,000 for western blots
SRSF1	Santa Cruz, sc-33652	1:200 for immunohistochemistry
SRSF1	Abcam, ab129108 for Fig. 1b	1:200 for immunofluorecence
SM-a-actin	Abcam, ab5694 for Fig. 1b	1:200 for immunofluorecence
PCNA	Cell Signaling Technology, 2586; recognizes the protein region within the amino acid residues 111–1251	1:200 for immunohistochemistry, 1:1,000 for western blots
p21	Cell Signaling Technology, 2947	1:1,000 for western blots
EGR1	Cell Signaling Technology, 4153	1:100 for immunoprecipitation, 1:1,000 for western blots
GFP	Cell Signaling Technology, 2955	1:1,000 for western blots
Myc	Sigma, SAb4700447	1:100 for immunoprecipitation, 1:1,000 for western blots
p53(CM1)	Vector Laboratories, VP-P955; a rabbit polyclonal antibody raised against recombinant full-length human p53 protein that recognizes all p53 isoforms, in which Δ133p53β and Δ133p53γ are weakly recognized as these isoforms have lost most immunogenic domains of p53	1:1,000 for western blots
β-actin	Sigma, A1978	1:1,000 for western blots
KLF5	Gene-Tex, GTX103289	1:1,000 for western blots
Bcl-xL	Cell Signaling Technology, 2762	1:1,000 for western blots
eIF-5	Santa Cruz, sc282	1:1,000 for western blots

Supplementary Table 3

Primers for real-time PCR

Genes	Sense primers (5'-3')	Antisense primers (5'-3')
h18S	CAGCCACCCGAGATTGAGCA	TAGTAGCGACGGGCGGTGTG
Human SRSF1	TCCAGACATCCGAACCAA	TACCCATCGTAATCATAGCC
Human KLF5	AGCAGCAATGGACACTCTT	GCCTTCCCAGGTACACTT
Human p21	GGAAGACCATGTGGACCTGT	GGCGTTTGGAGTGGTAGAAA
Human Δ133p53	ACTCTGTCTCCTTCCTCTTCCTACAG	GTGTGGAATCAACCCACAGCT
Human TAp53	CAGCCAAGTCTGTGACTTGCA	GTGTGGAATCAACCCACAGCT
Human Δ40p53	TGAGTGGATCCATTGGAAGG	GTCTGAAAGACAAGAGCAGAAAG
Human Bcl-xL	CTGACAGTGAATCTGATGA	GACAAGAATGCCAAGTTAG
m18S	GGAAGGGCACCACCAGGAGT	GCAGCCCCGGACATCTAAG
Mouse SRSF1	GTGGAAGCTGGCAGGACTTA	AGGCAGTTTCTCCCTCGTGA
Mouse KLF5	GGAAGTCCCGATAGACAAGC	GCGAATTAACTGGCAGAGTG
Mouse Bcl-xL	CAGCGGAGAGTTAATGTT	AGGCAATGACAATCTGAG
Mouse p21	TGGGCATGTCAGAAGTCTCG	CTCGCAGCTTTCCAATGCAC
r18S	GGAAGGGCACCACCAGGAGT	TGCAGCCCCGGACATCTAAG
Rat SRSF1	CTCCGAGTGGAAGCTGGCAGGACT	CACCAGTGCCATCTCGGTAAACA
Rat KLF5	TTGAAGCTGCAGTATGCCTG	CTGAGGCACTGTCTCGTCTG
Rat Bcl-xL	CAGTGGAGAGCTAATGTT	AGGCGATGACAATCTGAG
Rat p21	CAAAGTATGCCGTCGTCTGTTC	TCAAAGTTCCACCGTTCTCG

Supplementary Table 4

Sequences of siRNAs against SRSF1, Δ133p53, KLF5, and EGR1

Human SRSF1	siRNA1	Sense (5'-3')	GCAGAUGCAGUAGGCGUAA
		Antisense (5'-3')	UUACGCCUACUGCAUCUGC
	siRNA2	Sense (5'-3')	GCAGAGAGCAGUAAUCCAA
		Antisense (5'-3')	UUGGAUUACUGCUCUCUGC
Human Δ133p53	siRNA1	Sense (5'-3')	UGUUCACUUGUGCCCUGACUUUCAA
		Antisense (5'-3')	UUGAAAGUCAGGGCACAAGUGAACA
	siRNA2	Sense (5'-3')	CUUGUGCCCUGACUUUCAATT
		Antisense (5'-3')	UUGAAAGUCAGGGCACAAGTT
Human KLF5	siRNA1	Sense (5'-3')	GCAGACUGCAGUGAAACAA
		Antisense (5'-3')	UUGUUUCACUGCAGUCUGC
	siRNA2	Sense (5'-3')	GCAUCCACUACUGCGAUUA
		Antisense (5'-3')	UAAUCGCAGUAGUGGAUGC
Human EGR1	siRNA1	Sense (5'-3')	CCAACAGUGGCAACACCUU
		Antisense (5'-3')	AAGGUGUUGCCACUGUUGG
	siRNA2	Sense (5'-3')	GCCUAGUGAGCAUGACCAA
		Antisense (5'-3')	GCCUAGUGAGCAUGACCAA
Human PCNA	siRNA1	Sense (5'-3')	ACGCGGATACCTTGGCGCTAGTATT
		Antisense (5'-3')	UUTUCTUGCGCCUUGGTUTCCGCGT
	siRNA2	Sense (5'-3')	CCAGGAGAAAGTTTCAGACTATGAA
		Antisense (5'-3')	TTCUTUGTGTGUUUCTTTCTCCTGG

Supplementary Table 5

ChIP-PCR primers for EGR1 binding peaks

Genes	Sense primers (5'-3')	Antisense primers (5'-3')
P1 (nt-2722 to nt -2577)	CCACTGCCTCCTTCAAAC	CTTAGTCACTGGGCAACAC
P2 (nt-105 to nt -10)	TCTCCACCCTAATTCCC	GTTTGTACACAACTTCTCTG
P3 (nt-410 to nt -558)	GAGGAGTCCACCCGAAA	TGCTCAGCACCCTTGTA
P4 (nt-1475 to nt -1576)	GCAGCCGAATTAGAGCAA	TCCTTGGGACAGGCTAAA

Supplementary Table 6

Primers for amplification of human Δ133p53 isoforms by RT-PCR (nested PCR)

Primers name	**5'-3' sequence**
N1Δ133(F9)	TAGACGCCAACTCTCTCTAG
N1Δ133(R9)	GACGCACACCTATTGCAAGCAAGGGTTC
N2Δ133(F10)	CTAGTGGGTTGCAGGAGGTGCTTACAC
N2Δ133(R10)	ATGTCAGTCTGAGTCAGGCCCTTCTGTC
N2Δ133b(F11)	CTAGTGGGTTGCAGGAGGTGCTTACAC
N2Δ133b(R11)	TTTGAAAGCTGGTCTGGTCCTGA
N2Δ133g(F12)	CTAGTGGGTTGCAGGAGGTGCTTACAC
N2Δ133g(R12)	TCGTAAGTCAAGTAGCATCTGAAGG

Supplementary Table 7

Primers for quantitative amplification of human p53 isoforms by RT-qPCR

Primers name	**5'-3' sequence**
Δ133 (I4) F3	ACTCTGTCTCCTTCCTCTTCCTACAG
Δ133 (E5) R3	GTGTGGAATCAACCCACAGCT
p53alpha (E9) F4	AACCACTGGATGGAGAATATTTCAC
p53alpha (E10) R4	CAGCTCTCGGAACATCTCGAA
p53beta (E9) F5	AACCACTGGATGGAGAATATTTCAC
p53beta (E9b) R5	TCATAGAACCATTTTCATGCTCTCTT
p53gamma (E9) F6	AACCACTGGATGGAGAATATTTCAC
p53gamma (E9g) R6	TCAACTTACGACGAGTTTATCAGGAA